Regnase-1 Prevents Pulmonary Arterial Hypertension via mRNA Degradation of IL-6 and PDGF in Alveolar Macrophages

Running title: Regnase-1 Controls Pulmonary Hypertension

Ai Yaku, MD[1,2]; Tadakatsu Inagaki, PhD[3]; Ryotaro Asano, MD, PhD[3,4,5]; Makoto Okazawa, PhD[3]; Hiroyoshi Mori, MD, PhD[3]; Ayuko Sato, PhD[6]; Fabian Hia, PhD[1]; Takeshi Masaki, MD, PhD[3]; Yusuke Manabe, MD[3,7]; Tomohiko Ishibashi, MD, PhD [3]; Alexis Vandenbon, PhD[8]; Yoshinari Nakatsuka, MD, PhD[1]; Kotaro Akaki PhD[1]; Masanori Yoshinaga, MD, PhD[1]; Takuya Uehata, MD, PhD[1]; Takashi Mino PhD[1]; Satoshi Morita, PhD[9]; Hatsue Ishibashi-Ueda, MD, PhD[10]; Akio Morinobu, MD, PhD[2]; Tohru Tsujimura, MD, PhD[6]; Takeshi Ogo, MD, PhD[4,5]; Yoshikazu Nakaoka, MD, PhD[3, 11, 12]*; Osamu Takeuchi, MD, PhD[1]*

[1]Department of Medical Chemistry, Graduate School of Medicine, Kyoto University, Kyoto, Japan; [2]Department of Rheumatology and Clinical Immunology, Graduate School of Medicine, Kyoto University, Kyoto, Japan; [3]Department of Vascular Physiology, National Cerebral and Cardiovascular Center Research Institute, Suita, Japan; [4]Department of Advanced Medical Research for Pulmonary Hypertension, National Cerebral and Cardiovascular Center, Suita, Japan; [5]Department of Cardiovascular Medicine, National Cerebral and Cardiovascular Center, Suita, Japan; [6]Department of Pathology, Hyogo College of Medicine, Nishinomiya, Japan; [7]Department of Respiratory Medicine and Clinical Immunology, Osaka University Graduate School of Medicine, Suita, Japan; [8]Laboratory of Systems Virology, Department of Biosystems Science, Institute for Frontier Life and Medical Sciences, Kyoto University, Kyoto, Japan; [9]Department of Biomedical Statistics and Bioinformatics, Graduate School of Medicine, Kyoto University, Kyoto, Japan;

[10]Department of Pathology, National Cerebral and Cardiovascular Center, Suita, Japan; [11]Department of Cardiovascular Medicine, [12]Department of Molecular Imaging in Cardiovascular Medicine, Osaka University Graduate School of Medicine, Suita, Japan
*Y. Nakaoka and O. Takeuchi contributed equally.

Address of Correspondence:
Yoshikazu Nakaoka, MD, PhD
Department of Vascular Physiology, National Cerebral and Cardiovascular Center Research Institute, Kishibe-shimmachi, Suita, 564-8565, Japan
Phone:+81-6-6170-1070 Fax:+81-6-6170-1695
E-mail: ynakaoka@ncvc.go.jp

Osamu Takeuchi, MD, PhD
Department of Medical Chemistry, Graduate School of Medicine, Kyoto University
Yoshida-Konoe-cho, Sakyo-ku, Kyoto 606-8501, Japan.
Phone: +81-75-753-9500 Fax: +81-75-753-9502
E-mail: otake@mfour.med.kyoto-u.ac.jp

Abstract

Background: Pulmonary arterial hypertension (PAH) is a type of pulmonary hypertension (PH) characterized by obliterative pulmonary vascular remodeling, resulting in right heart failure. Although the pathogenesis of PAH is not fully understood, inflammatory responses and cytokines have been shown to be associated with PAH, particularly with connective tissue disease (CTD)-PAH. In this sense, Regnase-1, an RNase which regulates mRNAs encoding genes related to immune reactions, was investigated in relation to the pathogenesis of PH.

Methods: We first examined the expression levels of *ZC3H12A* (encoding Regnase-1) in peripheral blood mononuclear cells (PBMCs) from PH patients classified under various types of PH, searching for an association between the *ZC3H12A* expression and clinical features. We then generated mice lacking Regnase-1 in myeloid cells, including alveolar macrophages, and examined right ventricular systolic pressures (RVSP) and histological changes in the lung. We further performed a comprehensive analysis of the transcriptome of alveolar macrophages and pulmonary arteries to identify genes regulated by Regnase-1 in alveolar macrophages.

Results: *ZC3H12A* expression in PBMCs was inversely correlated with the prognosis and severity of PH patients, particularly in CTD-PAH. The critical role of Regnase-1 in controlling PAH was also reinforced by the analysis of mice lacking Regnase-1 in alveolar macrophages. These mice spontaneously developed severe PAH, characterized by the elevated RVSP and irreversible pulmonary vascular remodeling, which recapitulated the pathology of PAH patients. Transcriptomic analysis of alveolar macrophages and pulmonary arteries of these PAH mice revealed that *Il6*, *Il1b,* and *Pdgfa*/*b* are potential targets of Regnase-1 in alveolar macrophages in the regulation of PAH. The inhibition of Interleukin (IL)-6 by an anti-IL-6 receptor antibody or Platelet-derived growth factor (PDGF) by imatinib, but not IL-1β by anakinra, ameliorated the pathogenesis of PAH.

Conclusions: Regnase-1 maintains lung innate immune homeostasis via the control of IL-6 and PDGF in alveolar macrophages, thereby suppressing the development of PAH in mice. Furthermore, the decreased expression of Regnase-1 in various types of PH implies its involvement in PH pathogenesis and may serve as a disease biomarker as well as a therapeutic target for PH.

Key words: Regnase-1, macrophages, pulmonary hypertension, IL-6, PDGF

Non-standard Abbreviations and Acronyms: PAH, pulmonary arterial hypertension; mPAP, mean pulmonary arterial pressure; CTD, connective tissue disease; SSc, systemic sclerosis; PVOD, pulmonary veno-occlusive disease; PDGF, platelet-derived growth factor; RBP, RNA-binding protein; RVSP, right ventricular systolic pressure; 6MWD, 6-minute walk distance; αSMA, α-smooth muscle actin; vWF, von Willebrand factor

Clinical Perspective

What is new?

- We discovered that an RNase Regnase-1 is crucial for preventing severe PAH via the maintenance of alveolar macrophage homeostasis in mice.
- Regnase-1-mediated decay of mRNAs including IL-6 and PDGFs contributes to the inhibition of PAH development.
- Regnase-1 expression in PBMCs is inversely correlated with the prognosis and severity of PH patients, particularly CTD-PAH.

What are the clinical implications?

- Regnase-1 expression may serve as a PH disease biomarker.
- This study provides a unique mouse model for developing therapeutic approaches against severe CTD-PAH.
- Regnase-1 can be a therapeutic target for the treatment of PAH via the inhibition of a set of cytokines and growth factors.

Introduction

Pulmonary hypertension (PH) is defined by the increase of mean pulmonary arterial pressure (mPAP). PH is a devastating disease with the potential to cause right heart failure in addition to a high mortality rate.[1-4] PH is classified into five groups depending on underlying causes, including pulmonary arterial hypertension (PAH) (group 1), left heart disease (group 2), lung diseases or hypoxia (group 3), chronic thromboembolic pulmonary hypertension (CTEPH: group 4), and others (group 5). Among them, PAH is an especially fatal pulmonary vascular disease due to the excess proliferation of vascular smooth muscle cells and endothelial cells. PAH is a severe complication of connective tissue diseases (CTDs). In addition, pulmonary veno-occlusive disease (PVOD) is frequently associated with CTD-associated PAH (CTD-PAH),[5] especially in systemic sclerosis (SSc) patients.[6] Although the prognosis of PAH has improved due to the development of vasodilators, the prognosis of CTD-PAH remains poor.[7] One of the reasons for this is the lack of appropriate mouse models which recapitulate the pathophysiology of severe CTD-PAH patients.[8]

There are multiple growth factors that are potentially involved in PAH. These include platelet-derived growth factor (PDGF) and vascular endothelial growth factor (VEGF), as well as bone morphogenic proteins (BMPs).[4] Furthermore, circulating proinflammatory cytokines such as Interleukin (IL)-6, IL-1β, and tumor necrosis factor (TNF) are elevated in PAH patients.[9] Animal studies strongly support the contribution of cytokines, particularly through IL-6 signaling, in the pathogenesis of PAH.[10-15] These cytokines can be controlled by environmental factors through aryl hydrocarbon receptor, which is crucial for PAH development.[16]

Innate immune cells like macrophages are also crucial for the induction of PAH.[4] It is widely accepted that innate immune cells are the major producers of proinflammatory cytokines, whose expression is tightly regulated by transcriptional and posttranscriptional mechanisms.[17] In posttranscriptional regulation, immune reactions

are mediated by various RNA-binding proteins (RBPs) which control the translation and the decay of mRNAs involved in immune responses.[18, 19] Although the involvement of epigenetic and transcriptional regulations as well as microRNAs has been extensively studied,[4] the significance of RBPs in PAH is poorly understood.

Regnase-1 (encoded by the *ZC3H12A* gene) is an RBP playing a pivotal role in the posttranscriptional immune regulation in innate and acquired immune cells.[20, 21] Regnase-1 harbors an RNase domain, capable of degrading mRNAs involved in immune responses such as *Il6* and *Il1b* through the recognition of stem-loop structures in their 3' untranslated regions (3' UTR).[20, 22, 23] Regnase-1 initiates mRNA decay through a helicase, UPF1, following translation termination.[24] Regnase-1 deficiency in mice leads to the production of elevated levels of inflammatory cytokines, including IL-6, in macrophages and the development of severe autoimmune inflammatory diseases.[20, 23] Additionally, the lack of Regnase-1 in cardiomyocytes in mice resulted in the development of heart failure in response to pressure overload.[25] The expression of Regnase-1 has been implicated in various human diseases such as ulcerative colitis and pulmonary fibrosis.[26-28] However, it is not clear if Regnase-1 is involved in the pathogenesis of PAH.

In this study, we found that the expression levels of *ZC3H12A* in peripheral blood mononuclear cells (PBMCs) from PH patients were lower than those from healthy volunteers (HV). Furthermore, mice lacking Regnase-1 in myeloid cells spontaneously developed severe PAH.

Methods

All data and materials will be made available to researchers upon request. RNA sequencing data are publicly available at the DNA Data Bank of Japan (DRA013291, DRA013292). Clinical studies were approved by the Institutional Review Board of the National Cerebral and Cardiovascular Center, Suita, Japan (M30-060). Protocols of animal experiments were approved by the Kyoto University Animal Experimentation Committee (MedKyo21057) and by the National Cerebral and Cardiovascular Center Research Institute (18030, 19037, 20016 and 21068). A detailed description of the methods and supporting data are available in the Data Supplement.

Statistical analysis.

Data are presented as means ± standard deviation. Statistical analyses were performed using Graph Pad Prism 8, JMP version 15.2 and SAS version 9.4. Statistical significance was calculated with unpaired Student's t-test or One-way ANOVA with Tukey's multiple comparisons test, unless otherwise stated. Event-free survival curves were derived using Kaplan-Meyer method and were compared using log-rank test. Correlation analysis was performed with Pearson's linear correlation or Spearman's rank correlation. $P<0.05$ was considered statistically significant.

Results

Regnase-1 mRNA expression is decreased in PBMCs of PH patients

To investigate the involvement of Regnase-1 in PH, we examined the expression levels of *ZC3H12A* in PBMCs between PH patients (n=77) and age- and sex-matched HV (n=77) by reverse transcription-quantitative polymerase chain reaction (RT-qPCR) (Table 1). Hereafter, *ZC3H12A* indicates the Regnase-1 mRNA. Interestingly, *ZC3H12A* expression levels were significantly decreased in PH patients (Figure 1A). Immunoblot analysis revealed that Regnase-1 protein expression was also decreased in PBMCs from PH patients compared with HV (Figures S1A). We observed a correlation between Regnase-1 mRNA and its protein levels (Figure S1B), suggesting that the expression of Regnase-1 was controlled at the mRNA levels. The levels of *ZC3H12A* were lower even in PH patients who were categorized in World Health Organization-functional classes (WHO-FC) I and II, in addition to severe patients categorized in WHO-FC III and IV (Figure 1B and Table S1). When we divided PH patients into two groups based on *ZC3H12A* expression levels, patients expressing lower levels of *ZC3H12A* (n=40) showed significantly poor prognosis, exemplified by events such as death, lung transplantation, and hospitalization for right heart failure compared with those with higher levels of *ZC3H12A* (n=37) (Figure 1C and Table S2), suggesting that the expression levels of *ZC3H12A* are associated with the improved prognosis of PH patients. Consistently, *ZC3H12A* levels were negatively correlated with mPAP (Figure 1D). Moreover, PH patients with lower right ventricular ejection fraction (RVEF) expressed lower amounts of *ZC3H12A* (Figure 1E, Table S3 and S4). Furthermore, levels of PH biomarkers, brain natriuretic peptide (BNP) and uric acid (UA),[29, 30] were also inversely associated with *ZC3H12A* expression in PBMCs in PH patients (Figure 1F through 1H), suggesting that the expression level of *ZC3H12A* is inversely associated with the PH disease severity.

Since Regnase-1 is a regulator of inflammatory responses, we also checked the correlation between the expression of *ZC3H12A* and serum C-reactive protein (CRP) levels, a marker of inflammation. Interestingly, there was a negative correlation between *ZC3H12A* and CRP levels (Figure 1I and 1J). To analyze the association between the expression levels of *ZC3H12A* and treatment resistance, we divided PH patients who underwent PAH-specific medications into two groups based on the level of mPAP after treatment. The group with higher levels of mPAP showed significantly lower levels of *ZC3H12A* compared with those who were responsive to the therapies (Figure 1K). Taken together, these results suggest that lower expression levels of Regnase-1 are associated with poor prognosis, disease severity, inflammation, and treatment resistance.

Inverse correlation between the Regnase-1 expression in PBMCs and the severity of CTD-PAH

Next, we checked the expression levels of *ZC3H12A* in different groups of PH. We found that *ZC3H12A* levels were significantly decreased in various types of PH, including idiopathic and heritable PAH (I/HPAH), CTD-PAH (Table S5), congenital heart disease (CHD)-PAH, and even in CTEPH patients (Figure 2A). Whereas *ZC3H12A* expression levels were lower both in CTD-PAH and I/HPAH patients compared with HV irrespective of the WHO-functional classes (Figure 2B, 2C, Table S6 and S7), the negative correlation of *ZC3H12A* levels with mPAP was observed only in CTD-PAH, but not in I/HPAH, patients (Figure 2D). Similarly, the *ZC3H12A* expression levels tend to be correlated with the 6-minute walk distance (6MWD) in CTD-PAH, but not in I/HPAH, patients (Figure 2E). Nevertheless, UA levels were inversely correlated with *ZC3H12A* both in CTD-PAH and I/HPAH (Figure 2F), and patients with higher CRP levels also expressed lower levels of *ZC3H12A* both in CTD-PAH and I/HPAH patients (Figure 2G). These results clearly demonstrate that

ZC3H12A expression levels are decreased in PBMCs of various PH groups, and the levels are inversely correlated, particularly with the disease severity of CTD-PAH. To investigate whether *ZC3H12A* levels predict PH prognosis independent of other prognostic factors, we performed univariate and multivariate analyses. In the univariate analysis, *ZC3H12A* levels, age, BNP, and 6MWD were significantly associated with the PH prognosis (Table S8). Intriguingly, a series of multivariate analyses revealed that the *ZC3H12A* levels were the independent factor for PH prognosis against other factors (Table S8).

Spontaneous development of severe PAH in mice lacking Regnase-1 in myeloid cells

The aforementioned results prompted us to examine if Regnase-1 is also functionally involved in the pathogenesis of PAH by using mouse models. We hypothesized that Regnase-1 expressed in myeloid cells, which highly produce inflammatory cytokines, regulates PAH. Thus, we generated CD11c-Cre^{+}*Zc3h12a*$^{fl/fl}$ mice which lacked Regnase-1 in alveolar macrophages and conventional dendritic cells (cDCs) (Figure S2A). As the control of CD11c-Cre^{+}*Zc3h12a*$^{fl/fl}$ mice, we used the littermates with following genotypes: *Zc3h12a*$^{fl/+}$, *Zc3h12a*$^{fl/fl}$, or CD11c-Cre^{+}*Zc3h12a*$^{fl/+}$. To determine whether these mice developed PAH, we measured the right ventricular systolic pressure (RVSP) and the weight ratio of right ventricle (RV) to left ventricle (LV) plus septum (RV/(LV+S)). First, RVSP and the RV/(LV+S) ratio were comparable between *Zc3h12a*$^{fl/+}$ and CD11c-Cre^{+}*Zc3h12a*$^{fl/+}$ mice, suggesting that the presence of CD11c-Cre transgene did not cause hemodynamic changes (Figure S2B and S2C). In contrast, CD11c-Cre^{+}*Zc3h12a*$^{fl/fl}$ mice markedly elevated RVSP compared with control mice (Figure 3A). Age-dependent increases in the RV/(LV+S) ratio was also observed in CD11c-Cre^{+}*Zc3h12a*$^{fl/fl}$ mice (Figure 3B), suggesting the development of RV hypertrophy after week (wk) 9. Of note, there were no significant differences in RVSP

and the RV/(LV+S) ratio between male and female CD11c-Cre^{+}*Zc3h12a*$^{fl/fl}$ mice (Figure S2D and S2E). Hematoxylin and eosin (H&E) staining showed obstructive pulmonary arteries in CD11c-Cre^{+}*Zc3h12a*$^{fl/fl}$ mice (Figure 3C). Furthermore, extensive thickening of the medial and intimal wall of pulmonary arteries in CD11c-Cre^{+}*Zc3h12a*$^{fl/fl}$ mice was revealed by Elastica van Gieson (EVG) staining and immunohistochemistry analysis by staining α-smooth muscle actin (αSMA) and von Willebrand factor (vWF) (Figure 3C). In contrast, the presence of CD11c-Cre alone did not induce pulmonary arterial remodeling (Figure S2F). The pulmonary arterial occlusion rate was significantly elevated in CD11c-Cre^{+}*Zc3h12a*$^{fl/fl}$ mice (Figure 3D). In addition, CD11c-Cre^{+}*Zc3h12a*$^{fl/fl}$ mice showed various forms of vascular remodeling, including medial hypertrophy (Grade 1), partial neointimal thickening (Grade 2), occlusive neointimal thickening (≥75% occlusion) or fibrous intimal thickening (Grade 3) (Figure 3E and 3F). Interestingly, plexiform-like lesions (Grade 4) were observed under Regnase-1 deficiency (Figure 3F and Figure S2G). These results demonstrate that CD11c-Cre^{+}*Zc3h12a*$^{fl/fl}$ mice spontaneously develop severe PAH. Moreover, occlusion of pulmonary veins surrounded with inflammatory cells, a hallmark of PVOD, was observed in CD11c-Cre^{+}*Zc3h12a*$^{fl/fl}$ mice (Figure 3G). Histological analysis also revealed a massive infiltration of immune cells in the lungs, especially around the pulmonary arteries of CD11c-Cre^{+}*Zc3h12a*$^{fl/fl}$ mice (Figure 3C and 3F). We also observed cardiac fibrosis and infiltration of immune cells to the right and left ventricles of CD11c-Cre^{+}*Zc3h12a*$^{fl/fl}$ mice (Figure S3A). Furthermore, the infiltration of immune cells was observed in the liver and kidney (Figure S3B). CD11c-Cre^{+}*Zc3h12a*$^{fl/fl}$ mice produced anti-double-stranded DNA antibodies and exhibited early mortality (Figure S3C and S3D), indicating that CD11c-Cre^{+}*Zc3h12a*$^{fl/fl}$ mice develop an autoimmune inflammatory disease.

Regnase-1 was deleted in alveolar macrophages and cDCs, but not interstitial macrophages, in CD11c-Cre^{+}*Zc3h12a*$^{fl/fl}$ mice (Figure S2A). The numbers of CD103^{+}

cDC1 and CD11b^{+} cDC2, as well as interstitial macrophages, neutrophils, and T cells, but not alveolar macrophages, were increased in the lungs of CD11c-Cre^{+}*Zc3h12a*$^{fl/fl}$ mice (Figure S4A). However, the expression of co-stimulatory molecules CD40 and CD80 or the expression of cytokines like *Il1b* and *Il6,* which are already known to be targets of Regnase-1, were not augmented in cDCs from CD11c-Cre^{+}*Zc3h12a*$^{fl/fl}$ mice (Figure S4B and S4C). Interstitial macrophages from control and CD11c-Cre^{+}*Zc3h12a*$^{fl/fl}$ mice also expressed *Il1b* and *Il6* at similar levels (Figure S4D). In contrast, the lack of Regnase-1 resulted in the robust elevation of these cytokine genes in alveolar macrophages (Figure S4E) and of IL-6 concentrations in bronchoalveolar lavage fluid (BALF) samples (Figure S4F), suggesting that alveolar macrophages were activated under Regnase-1 deficiency.

To further investigate the myeloid cell types responsible for the development of PAH under Regnase-1 deficiency, we generated *LysM*$^{Cre/+}$*Zc3h12a*$^{fl/fl}$ mice in which Regnase-1 was depleted in alveolar and interstitial macrophages in the lung (Figure S5A). As the control of *LysM*$^{Cre/+}$*Zc3h12a*$^{fl/fl}$ mice, we used *Zc3h12a*$^{fl/+,}$ *Zc3h12a*$^{fl/fl}$, or *LysM*$^{Cre/+}$*Zc3h12a*$^{fl/+}$ mice, because we did not find any significant difference in RVSP, the RV/(LV+S) ratio or histological changes in pulmonary arteries (Figure S5B through S5D). Regnase-1 deletion resulted in the increase of cytokines like *Il6* and *Il1b* in macrophages, and elevated IL-6 concentration in BALF, and the accumulation of various immune cells except for alveolar macrophages in the lung (Figure S5E through S5H). Consistent with a previous report,[31] organs like the liver and kidney of *LysM*$^{Cre/+}$*Zc3h12a*$^{fl/fl}$ mice were infiltrated with immune cells (Figure S6A). *LysM*$^{Cre/+}$*Zc3h12a*$^{fl/fl}$ mice exhibited higher mortality compared with control mice (Figure S6B). Intriguingly, these mice also spontaneously developed PAH as characterized by the increase of RVSP and occlusion rate of pulmonary arteries as well as arterial remodeling at 13 wk (Figure 3H through 3K). Although the RV/(LV+S) ratio was not altered at this age, it was significantly increased in *LysM*$^{Cre/+}$*Zc3h12a*$^{fl/fl}$ mice

20 wk after birth (Figure 3I). Significant hemodynamic changes were not observed between male and female *LysM*$^{Cre/+}$*Zc3h12a*$^{fl/fl}$ mice (Figure S6C and S6D). The profound pathological changes of pulmonary arteries were observed consistently in 20 wk old *LysM*$^{Cre/+}$*Zc3h12a*$^{fl/fl}$ mice lungs characterized by a myriad of forms of vascular remodeling corresponding to grades 1 to 4 (Figure 3K, Figure 3L and Figure S6E) as well as the characteristics of PVOD (Figure 3M). Cardiac fibrosis and immune cell infiltration were found in the right and left ventricles of *LysM*$^{Cre/+}$*Zc3h12a*$^{fl/fl}$ mice (Figure S6F). These results demonstrate that mice lacking Regnase-1 in macrophages, but not DCs, similarly developed PAH related to CTD. Since the lack of Regnase-1 in alveolar macrophages was a common point between these two strains of mice, we hypothesized that the lack of Regnase-1 in alveolar macrophages is responsible for the development of PAH.

Regnase-1 expression in myeloid cells contributes to the development of PAH under hypoxic conditions

Currently established mouse models of PH are induced by exposure to hypoxia or by exposure to hypoxia in combination with the injection of Sugen 5416, an inhibitor of the VEGF receptor.[32] To elucidate if Regnase-1 in myeloid cells is involved in the pathogenesis of hypoxia-induced PH in mice, we first investigated the effects of hypoxia in CD11c-Cre^{+}*Zc3h12a*$^{fl/+}$ mice. Whereas mice with Regnase-1 haploinsufficiency in myeloid cells did not spontaneously develop PH (Figure S2B thorough S2C), exposure of CD11c-Cre^{+}*Zc3h12a*$^{fl/+}$ mice to hypoxia resulted in an increase of RVSP and PA occlusion rates, but not the RV/(LV+S) ratio compared with control *Zc3h12a*$^{fl/+}$ mice (Figure 4A through 4C). Similarly, RVSP and PA occlusion rates were higher in hypoxia-treated *LysM*$^{Cre/+}$*Zc3h12a*$^{fl/+}$ mice compared to control *Zc3h12a*$^{fl/+}$ mice, although the RV/(LV+S) ratio was comparable (Figure 4D through 4F). These results indicated that the Regnase-1 in myeloid cells is also involved in the

prevention of PH caused by hypoxic conditions. Of note, haploinsufficiency of Regnase-1 in alveolar macrophages is a common feature in both mouse models, supporting the potential role of Regnase-1 in alveolar macrophages in controlling the development of PAH even under hypoxic conditions.

Regnase-1-deficiency in alveolar macrophages contributes to the promotion of PAH

Besides innate immune cells, we also investigated the contribution of lymphocytes in the control of PAH pathogenesis. Indeed, deletion of Regnase-1 in myeloid cells in CD11c-Cre^{+}*Zc3h12a*$^{fl/fl}$ or *LysM*$^{Cre/+}$*Zc3h12a*$^{fl/fl}$ mice led to the infiltration of not only monocytes/macrophages but also T cells and B cells to the lung (Figure S4A and S5H). In the lung, T and B cells accumulated around remodeled pulmonary arteries (Figure S7A), whereas macrophages were rarely present close to pulmonary arteries and majorly localized in the alveoli coexpressing CD11c (Figure S7B). To investigate the contribution of acquired immune cells to the remodeling of pulmonary arteries, we crossed CD11c-Cre^{+}*Zc3h12a*$^{fl/fl}$ with *Rag2*$^{-/-}$ mice which lack T and B cells. We found a mild increase of RVSP without affecting the RV/(LV+S) ratio and occlusive pulmonary arterial remodeling in CD11c-Cre^{+}*Zc3h12a*$^{fl/fl}$*Rag2*$^{-/-}$ mice compared with control mice (Figure 4G through 4I). Whereas the severity of histological changes was much less in CD11c-Cre^{+}*Zc3h12a*$^{fl/fl}$*Rag2*$^{-/-}$ mice compared with the same age (16 wk) of CD11c-Cre^{+}*Zc3h12a*$^{fl/fl}$ mice (Figure 4J), CD11c-Cre^{+}*Zc3h12a*$^{fl/fl}$*Rag2*$^{-/-}$ mice with 8 months developed severe pulmonary vascular remodeling such as grade 4, similar to those seen in CD11c-Cre^{+}*Zc3h12a*$^{fl/fl}$ mice (Figure 4K). We also found cardiac fibrosis in CD11c-Cre^{+}*Zc3h12a*$^{fl/fl}$*Rag2*$^{-/-}$ mice (Figure S8A), although fibrotic changes were milder than CD11c-Cre^{+}*Zc3h12a*$^{fl/fl}$ and *LysM*$^{Cre/+}$*Zc3h12a*$^{fl/fl}$ mice. In contrast, other organs such as the liver and kidney did not show histological changes under lymphocyte deficiency (Figure S8B), suggesting myeloid cells lacking Regnase-1 specifically

induced lung and heart pathology under lymphocytes deficiency. These results indicate that both lymphocyte-dependent and -independent mechanisms contribute to the pathogenesis of PAH under Regnase-1 deficiency in myeloid cells.

To clarify the contribution of alveolar macrophages in the development of PAH under Regnase-1 deficiency, we depleted alveolar macrophages by intratracheal treatment of CD11c-Cre^{+}*Zc3h12a*$^{fl/fl}$*Rag2*$^{-/-}$ mice or control *Rag2*$^{-/-}$ mice with clodronate liposomes (CL) twice a week (Figure 4L). Flow cytometry analysis of the lungs revealed the successful depletion of alveolar, but not interstitial, macrophages with CL treatment in both control and CD11c-Cre^{+}*Zc3h12a*$^{fl/fl}$*Rag2*$^{-/-}$ mice (Figure 4M and Figure S8C). CL treatment significantly improved the occlusion rate of pulmonary arteries in CD11c-Cre^{+}*Zc3h12a*$^{fl/fl}$*Rag2*$^{-/-}$ mice (Figure 4N and 4O), further confirming that alveolar macrophages lacking Regnase-1 trigger vascular remodeling in mice, leading to the development of PAH.

Analysis of ligand-target linkage between alveolar macrophages lacking Regnase-1 and pulmonary arteries

To uncover the mechanisms of how pulmonary arterial remodeling is induced by alveolar macrophages under Regnase-1 deficiency, we performed transcriptomic analyses of pulmonary arteries obtained from CD11c-Cre^{+}*Zc3h12a*$^{fl/fl}$ and control lung sections by laser capture microdissection (Figure 5A). As expected, gene set enrichment analysis (GSEA) showed that gene sets involved in cell cycle and cell proliferation were highly enriched in genes upregulated in pulmonary arteries from CD11c-Cre^{+}*Zc3h12a*$^{fl/fl}$ mice (Figure 5B), consistent with the thickening of medial walls and concentric laminar neointima. Also, gene ontology (GO) analysis revealed that biological processes related to immune responses were highly enriched in genes upregulated in pulmonary arteries from CD11c-Cre^{+}*Zc3h12a*$^{fl/fl}$ mice compared with control mice (Figure 5C). Furthermore, KEGG pathway analysis revealed that genes in

the cytokine-cytokine receptor interaction pathway were highly enriched in CD11c-Cre^{+}*Zc3h12a*$^{fl/fl}$ pulmonary arteries (Figure 5D).

We also analyzed transcriptomic changes in alveolar macrophages sorted from CD11c-Cre^{+}*Zc3h12a*$^{fl/fl}$ and control mice (Figure 5A). The transcriptomic analysis of alveolar macrophages showed an upregulation of various genes involved in macrophage activation towards both M1 and M2 profiles (Figure 5E). These genes included *Il6*, *Nos2*, *Chil3*, *Arg1,* and *Mrc1*. In addition, various growth factors and cytokines were upregulated in alveolar macrophages of CD11c-Cre^{+}*Zc3h12a*$^{fl/fl}$ mice (Figure 5F).

These results prompted us to hypothesize that factor(s) secreted by Regnase-1-deficient alveolar macrophages control the proliferation of pulmonary arterial cells, thereby inducing vascular remodeling. To analyze the relationship in transcriptomic changes between alveolar macrophages and pulmonary arteries, we analyzed the data using NicheNet, a computational method which predicts ligand-target links by combining the transcriptome data of alveolar macrophages and pulmonary arteries[33]. The analysis identified a set of ligand-target networks potentially operating between Regnase-1-deficient macrophages and pulmonary arteries (Figure 5G). Particularly high-ranked ligands include *Il1b, Il1a*, *Tnfsf10*, *Il6*, *Vegfa*, *Pdgfb*, *Il33*, *Apoe*, *Anxa1*, and *Ccl5* (Figure 5G). Importantly, these growth factors and cytokines produced from Regnase-1-deficient alveolar macrophages may contribute to the pathological changes in pulmonary arteries.

Coordinated regulation of IL-6 and PGDF by Regnase-1 in alveolar macrophages

We next analyzed if the factors identified by the NicheNet are directly regulated by Regnase-1-mediated mRNA decay. Since Regnase-1 recognizes 3' UTR of target mRNAs, we generated luciferase reporter constructs harboring the 3' UTR regions of *Il1a*, *Tnfsf10*, *Vegfa*, *Pdgfb*, *Il33*, *Apoe*, *Anxa1* and *Ccl5*, as well as prominent growth factors *Pdgfa*, *Egf* and *Igf1*. In addition to a validated Regnase-1 target 3'UTR, *Il6*, the

overexpression of wild-type Regnase-1 (Reg1 WT) significantly suppressed luciferase activity in the presence of the 3' UTRs for *Il1a*, *Tnfsf10*, *Pdgfa*, *Pdgfb* and *Il33*, but not *Vegfa*, *Apoe*, *Anxa1*, *Ccl5*, *Egf* or *Igf1* in HEK293T cells (Figure 6A). In contrast, nuclease-inactive mutant Regnase-1 (D141N) failed to inhibit the reporter activity in any genes tested (Figure 6A), indicating that Regnase-1 functions as the RNase to control these novel target mRNAs. Thus, the results demonstrate that not only *Il6* and *Il1b*, but also *Il1a*, *Il33*, *Tnfsf10, Pdgfa,* and *Pdgfb* are the targets of Regnase-1 in alveolar macrophages, potently associated with the development of PAH.

Inhibition of IL-6 and PGDF alleviated PAH induced by Regnase-1 deficiency

We next explored what factor(s) are involved in the pathogenesis of PAH under Regnase-1 deficiency in alveolar macrophages. Since IL-6 is an inflammatory cytokine closely associated with the pathogenesis of PAH and is elaborately regulated by Regnase-1, we first evaluated the contribution of IL-6 in the PAH pathogenesis by treating CD11c-Cre^{+}*Zc3h12a*$^{fl/fl}$ mice with an anti-IL-6R antibody, MR16-1 or control IgG (Figure 6B). IL-6 blockade with MR16-1 significantly attenuated RVSP as well as the RV/(LV+S) ratio in CD11c-Cre^{+}*Zc3h12a*$^{fl/fl}$ mice (Figure 6C and 6D), indicating that Regnase-1-mediated regulation of IL-6 is involved in disease pathogenesis. However, histological analysis revealed that the occlusion of pulmonary arteries and the frequency of severely remodeled pulmonary arteries (Grade 3) in CD11c-Cre^{+}*Zc3h12a*$^{fl/fl}$ mice were decreased but not completely alleviated following MR16-1 treatment (Figure 6E through 6G), implying that factors other than IL-6 contribute to the development of PAH. To investigate the IL-6-indepedent mechanisms involved in the pathogenesis of PAH under Regnase-1 deficiency, we focused on the control of the signaling of IL-1 and PDGF, whose mRNAs are directly regulated by Regnase-1 (Figure 6A). IL-1-mediated responses are known to be inhibited by the treatment with IL-1 receptor antagonist (anakinra) *in vivo.*[34] Additionally, the inhibition of PDGF

signaling is mediated by imatinib, the tyrosine kinase inhibitor that suppresses both PDGF receptors (PDGFR)-α and -β.[35, 36]Whereas the daily intraperitoneal treatment with anakinra failed to suppress RVSP, daily oral treatment with imatinib significantly decreased RVSP in CD11c-Cre^{+}*Zc3h12a*$^{fl/fl}$ mice (Figure 6H and 6I). Nevertheless, the RV/(LV+S) ratio was not significantly altered even in response to the treatment with imatinib (Figure 6J). Histologically, the occlusion rate of pulmonary arteries was significantly decreased in CD11c-Cre^{+}*Zc3h12a*$^{fl/fl}$ mice treated with imatinib (Figure 6K and 6L). Furthermore, the decrease of severely remodeled arteries was observed in imatinib treated mice (Figure 6M). On the other hand, anakinra treatment did not significantly improve the occlusion or remodeling of pulmonary arteries (Figure 6K through 6M).

Discussion

In this study, we discovered that Regnase-1 is critical for the pathogenesis of PAH. The expression of *ZC3H12A* in PBMCs was decreased in PH patients and inversely associated with the severity of CTD-PAH. Mice lacking Regnase-1 in myeloid cells spontaneously developed severe PAH. We identified a set of Regnase-1-target mRNAs in alveolar macrophages which potentially contribute to the pathogenesis of PAH. Among them, inhibition of IL-6 and PDGF alleviated the PAH caused by Regnase-1 deficiency in alveolar macrophages. Taken together, Regnase-1 prevents the development of PAH by degrading mRNAs including *Il6* and *Pdgfa/b* in alveolar macrophages (Figure S9).

There are few severe PAH models in mice, which mimic intimal cell proliferation and complex plexiform-like lesions observed in severe PAH in patients,[8] except for models affecting hypoxia/hypoxia-responsive pathways. Although Sugen5416/hypoxia treatment is a widely-used severe PAH animal model for rats,[37, 38] mice treated with Sugen5416/hypoxia exhibit muscularization of the media but not severe intimal cell proliferation.[8] Further, endothelial cell-specific Prolyl-4 hydroxylase 2-deficient mice were reported to exhibit severe PAH via hypoxia-inducible factor-2α.[39, 40] Mouse models of *Schistosoma*-associated PAH also cause severe inflammatory PAH, although the mice were not fatal and Schistosomiasis can be resolved.[41] Interestingly, mice lacking Regnase-1 in myeloid cells by using CD11c-Cre or *Lys*M^{Cre} mice spontaneously develop irreversible PAH with concentric intimal wall thickening and complex plexiform-like lesions under normoxic conditions. Moreover, these mice presented with PVOD and cardiac fibrosis, which are often associated with CTD-PAH. To the best of our knowledge, these mice represent a novel mouse model which better recapitulates the pathophysiology of severe CTD-PAH patients, as compared to existing mouse models.

Occlusion of pulmonary arteries observed in mice lacking Regnase-1 in myeloid cells was ameliorated by depleting alveolar macrophages by clodronate treatment. The results suggest that Regnase-1 in alveolar macrophages contributes to the development of PAH, at least in part by its interaction with pulmonary arterial cells. We have previously shown that Regnase-1 suppresses mRNAs like *Il6* and *Il12b* in macrophages stimulated with Toll-like receptor (TLR) ligands.[20] Consistently, alveolar macrophages lacking Regnase-1 also expressed high levels of *Il6* and *Il1b*, although the increase was not so apparent in Regnase-1-deficient DCs or interstitial macrophages. Noteworthy, the expression of *Pdgfb* was elevated in alveolar, but not interstitial, macrophages under Regnase-1 deficiency (Figure S10). The reason for the difference in the contribution of Regnase-1 in myeloid and other cell types requires further studies using conditional deletion of Regnase-1 using Cre mouse strains expressing in various immune cell types. However, it is tempting to speculate that alveolar macrophages are more likely to be exposed to environmental factors like pathogen-associated molecular patterns (PAMPs) and damage-associated molecular patterns (DAMPs),[42] which require Regnase-1 to maintain homeostasis.

The integrated analysis of transcriptome data sets of alveolar macrophages and pulmonary arteries identified potential ligands produced by alveolar macrophages under Regnase-1 deficiency. Among them, *Il1b*, *Il1a*, *Tnfsf10*, *Il6*, *Vegfa*, *Pdgfb*, *Il33*, *Apoe,* and *Anxa1* were identified as ligands which may affect the pulmonary vascular remodeling. In addition to already validated targets of Regnase-1-mediated mRNA decay like *Il6* and *Il1b*,[20, 23] we found that even growth factors like *Pdgfb* as well as *Pdgfa* can be directly regulated by Regnase-1-mediated mRNA decay. The importance of IL-6 in the pathogenesis of PAH was documented by a study generating mice overexpressing IL-6 under a Clara cell-specific promoter.[13] The IL-6 transgenic mice developed PAH with modest neointimal lesions, which was worsened in hypoxia. Considering the similarity between Regnase-1-deficient and IL-6 transgenic mice, IL-6

might promote the progression of neointimal lesions under Regnase-1 deficiency. Indeed, the inhibition of IL-6 signaling alleviated the progression of PAH and neointimal lesions under Regnase-1 deficiency.

Blocking IL-6 or PDGF signaling alleviated but not completely normalized hemodynamical and pathological changes in mice lacking Regnase-1 in myeloid cells. Although the effect of anakinra was not observed in this study, we cannot exclude the possibility that this is because of the incomplete inhibition of the IL-1R signaling. The development of more effective ways to block the IL-1R will clarify their contribution. Furthermore, it is plausible that additional mRNAs are controlled by Regnase-1 in alveolar macrophages in the prevention of PAH progression. TNF-related apoptosis-inducing ligand (TRAIL), encoded in the *Tnfsf10* gene, is one of such candidates (Figure 5G and 6A). Indeed, TRAIL was shown to be expressed in PAH pulmonary vascular lesions and mediate pathogenesis of PH in mice induced by hypoxia and various drug-induced PAH models.[43] Further studies are required to clarify the contribution of TRAIL in the pathogenesis of PAH under Regnase-1 deficiency. Furthermore, M2-like macrophage polarization has been proposed to promote PAH,[10] which was also observed in Regnase-1 lacking alveolar macrophages. Additionally, CD11c-Cre^{+}*Zc3h12a*$^{fl/fl}$*Rag2*$^{-/-}$ mice developed mild PAH compared with that of CD11c-Cre^{+}*Zc3h12a*$^{fl/fl}$ mice of the same age, suggesting that activated lymphocytes partially contribute to the development of PAH. Thus, Regnase-1 acts as a hub for the control of alveolar macrophages in preventing the pathogenesis of PAH by degrading mRNAs for cytokines and growth factors.

The expression of Regnase-1 mRNA was decreased not only in CTD-PAH but also in various PH groups, including I/HPAH and even CTEPH, consistent with Regnase-1 being an inflammatory regulator critical for autoimmune diseases. The general contribution of Regnase-1 in PH is also implicated by the data showing

exacerbation of hypoxia-induced PH under Regnase-1 haploinsufficiency in myeloid cells in mice.

An open question is the mechanisms by which Regnase-1 mRNA expression is controlled in PBMCs depending on PH pathogenesis. We have previously shown that the Regnase-1 protein undergoes posttranslational modification, including phosphorylation-induced degradation or 14-3-3-mediated sequestration and MALT1-mediated cleavage downstream of the TLR and antigen-receptor signaling pathways, respectively.[23, 44-46] Regnase-1 mRNA is also known to be controlled transcriptionally and post-transcriptionally i.e. through self-regulation.[45] Given that the expression of Regnase-1 is tightly correlated with the severity of CTD-PAH, immune cell activation might be responsible for the changes in Regnase-1 expression. Nevertheless, further studies will uncover the mechanisms of how Regnase-1 expression is suppressed in PH patients, which can be important for the uncovering of the cause of PH, including PAH.

In summary, this study clearly demonstrated that Regnase-1 is both clinically and experimentally associated with the pathogenesis of PAH. Regnase-1 in myeloid cells, especially alveolar macrophages, is a key regulator of a variety of cytokines and growth factors. As such, Regnase-1 could serve as a novel therapeutic target in the control of PH, including PAH. The development of strategies upregulating Regnase-1 activity might be an ideal therapy for PH.

Acknowledgments

We thank Keiko Ohta-Ogo for discussions and Yoshimi Okumoto for secretarial assistance, Yukari Sando and Takefumi Kondo for RNA sequencing and the Center for Anatomical, Pathological and Forensic Medical Research, Kyoto University for preparing microscope slides.

Sources of Funding

This research was supported by a Grant-in-Aid for Scientific Research (S) (18H05278, to O.T.) and Japan Agency for Medical Research and Development (AMED) under Grant Numbers JP19gm4010002 and JP21ae0121030 (to O.T.), and JP22ek0109592 (to Y.Nakaoka), and by Takeda Science Foundation (to Y.Nakaoka), Grant-in-Aid for Japan Society for the Promotion of Science (JSPS) Research Fellow, GlaxoSmithKline Japan Research Grant 2019, and Fujiwara memorial foundation (to A.Y.), Kanae Foundation, SENSHIN Medical Research Foundation, Ichiro Kanehara Foundation, and Osaka Heart Club (to T.Masaki).

Disclosures

None.

Supplemental Materials

Supplemental Methods

Supplemental Figures S1-S10

Supplemental Tables S1-S8

References 47-55

References

1. Galie N, Humbert M, Vachiery JL, Gibbs S, Lang I, Torbicki A, Simonneau G, Peacock A, Noordegraaf AV, Beghetti M, Ghofrani A, Sanchez MAG, Hansmann G, Klepetko W, Lancellotti P, Matucci M, McDonagh T, Pierard LA, Trindade PT, Zompatori M, Hoeper M, ESC ESC and ERS ERS. 2015 ESC/ERS Guidelines for the diagnosis and treatment of pulmonary hypertension The Joint Task Force for the Diagnosis and Treatment of Pulmonary Hypertension of the European Society of Cardiology (ESC) and the European Respiratory Society (ERS) Endorsed by: Association for European Paediatric and Congenital Cardiology (AEPC), International Society for Heart and Lung Transplantation (ISHLT). *Eur Heart J*. 2016;37:67-+.
2. Hassoun PM. Pulmonary Arterial Hypertension. *N Engl J Med*. 2021;385:2361-2376.
3. Rabinovitch M, Guignabert C, Humbert M and Nicolls MR. Inflammation and immunity in the pathogenesis of pulmonary arterial hypertension. *Circ Res*. 2014;115:165-75.
4. Thenappan T, Ormiston ML, Ryan JJ and Archer SL. Pulmonary arterial hypertension: pathogenesis and clinical management. *BMJ*. 2018;360:j5492.
5. Montani D, Lau EM, Dorfmuller P, Girerd B, Jais X, Savale L, Perros F, Nossent E, Garcia G, Parent F, Fadel E, Soubrier F, Sitbon O, Simonneau G and Humbert M. Pulmonary veno-occlusive disease. *Eur Respir J*. 2016;47:1518-34.
6. Overbeek MJ, Vonk MC, Boonstra A, Voskuyl AE, Vonk-Noordegraaf A, Smit EF, Dijkmans BA, Postmus PE, Mooi WJ, Heijdra Y and Grunberg K. Pulmonary arterial hypertension in limited cutaneous systemic sclerosis: a distinctive vasculopathy. *Eur Respir J*. 2009;34:371-9.
7. Rubenfire M, Huffman MD, Krishnan S, Seibold JR, Schiopu E and McLaughlin VV. Survival in Systemic Sclerosis With Pulmonary Arterial Hypertension Has Not Improved in the Modern Era. *Chest*. 2013;144:1282-1290.
8. Gomez-Arroyo J, Saleem SJ, Mizuno S, Syed AA, Bogaard HJ, Abbate A, Taraseviciene-Stewart L, Sung Y, Kraskauskas D, Farkas D, Conrad DH, Nicolls MR and Voelkel NF. A brief overview of mouse models of pulmonary arterial hypertension: problems and prospects. *Am J Physiol Lung Cell Mol Physiol*. 2012;302:L977-91.
9. Soon E, Holmes AM, Treacy CM, Doughty NJ, Southgate L, Machado RD, Trembath RC, Jennings S, Barker L, Nicklin P, Walker C, Budd DC, Pepke-Zaba J and Morrell NW. Elevated levels of inflammatory cytokines predict survival in

idiopathic and familial pulmonary arterial hypertension. *Circulation*. 2010;122:920-7.

10. Hashimoto-Kataoka T, Hosen N, Sonobe T, Arita Y, Yasui T, Masaki T, Minami M, Inagaki T, Miyagawa S, Sawa Y, Murakami M, Kumanogoh A, Yamauchi-Takihara K, Okumura M, Kishimoto T, Komuro I, Shirai M, Sakata Y and Nakaoka Y. Interleukin-6/interleukin-21 signaling axis is critical in the pathogenesis of pulmonary arterial hypertension. *P Natl Acad Sci USA*. 2015;112:E2677-E2686.
11. Mickael C, Kumar R, Hernandez-Saavedra D, Kassa B, Sanders L, Koyanagi D, Gu S, Lee MH, Tuder RM and Graham BB. IL-6Ra in Smooth Muscle Cells Protects against Schistosoma- and Hypoxia-induced Pulmonary Hypertension. *Am J Respir Cell Mol Biol*. 2019;61:123-126.
12. Savale L, Tu L, Rideau D, Izziki M, Maitre B, Adnot S and Eddahibi S. Impact of interleukin-6 on hypoxia-induced pulmonary hypertension and lung inflammation in mice. *Respir Res*. 2009;10:6.
13. Steiner MK, Syrkina OL, Kolliputi N, Mark EJ, Hales CA and Waxman AB. Interleukin-6 overexpression induces pulmonary hypertension. *Circ Res*. 2009;104:236-44, 28p following 244.
14. Tamura Y, Phan C, Tu L, Le Hiress M, Thuillet R, Jutant EM, Fadel E, Savale L, Huertas A, Humbert M and Guignabert C. Ectopic upregulation of membrane-bound IL6R drives vascular remodeling in pulmonary arterial hypertension. *J Clin Invest*. 2018;128:1956-1970.
15. Mori H, Ishibashi T, Inagaki T, Okazawa M, Masaki T, Asano R, Manabe Y, Ohta-Ogo K, Narazaki M, Ishibashi-Ueda H, Kumanogoh A and Nakaoka Y. Pristane/Hypoxia (PriHx) Mouse as a Novel Model of Pulmonary Hypertension Reflecting Inflammation and Fibrosis. *Circ J*. 2020;84:1163-1172.
16. Masaki T, Okazawa M, Asano R, Inagaki T, Ishibashi T, Yamagishi A, Umeki-Mizushima S, Nishimura M, Manabe Y, Ishibashi-Ueda H, Shirai M, Tsuchimochi H, Pearson JT, Kumanogoh A, Sakata Y, Ogo T, Kishimoto T and Nakaoka Y. Aryl hydrocarbon receptor is essential for the pathogenesis of pulmonary arterial hypertension. *P Natl Acad Sci USA*. 2021;118.
17. Takeuchi O and Akira S. Pattern recognition receptors and inflammation. *Cell*. 2010;140:805-20.
18. Anderson P. Post-transcriptional regulons coordinate the initiation and resolution of inflammation. *Nature Reviews Immunology*. 2010;10:24-35.
19. Carpenter S, Ricci EP, Mercier BC, Moore MJ and Fitzgerald KA. Post-transcriptional regulation of gene expression in innate immunity. *Nat Rev Immunol*.

2014;14:361-76.

20. Matsushita K, Takeuchi O, Standley DM, Kumagai Y, Kawagoe T, Miyake T, Satoh T, Kato H, Tsujimura T, Nakamura H and Akira S. Zc3h12a is an RNase essential for controlling immune responses by regulating mRNA decay. *Nature*. 2009;458:1185-U124.
21. Mino T and Takeuchi O. Regnase-1-related endoribonucleases in health and immunological diseases. *Immunol Rev*. 2021;304:97-110.
22. Mino T, Murakawa Y, Fukao A, Vandenbon A, Wessels HH, Ori D, Uehata T, Tartey S, Akira S, Suzuki Y, Vinuesa CG, Ohler U, Standley DM, Landthaler M, Fujiwara T and Takeuchi O. Regnase-1 and Roquin Regulate a Common Element in Inflammatory mRNAs by Spatiotemporally Distinct Mechanisms. *Cell*. 2015;161:1058-1073.
23. Uehata T, Iwasaki H, Vandenbon A, Matsushita K, Hernandez-Cuellar E, Kuniyoshi K, Satoh T, Mino T, Suzuki Y, Standley DM, Tsujimura T, Rakugi H, Isaka Y, Takeuchi O and Akira S. Malt1-induced cleavage of regnase-1 in CD4(+) helper T cells regulates immune activation. *Cell*. 2013;153:1036-49.
24. Mino T, Iwai N, Endo M, Inoue K, Akaki K, Hia F, Uehata T, Emura T, Hidaka K, Suzuki Y, Standley DM, Okada-Hatakeyama M, Ohno S, Sugiyama H, Yamashita A and Takeuchi O. Translation-dependent unwinding of stem-loops by UPF1 licenses Regnase-1 to degrade inflammatory mRNAs. *Nucleic Acids Res*. 2019;47:8838-8859.
25. Omiya S, Omori Y, Taneike M, Murakawa T, Ito J, Tanada Y, Nishida K, Yamaguchi O, Satoh T, Shah AM, Akira S and Otsu K. Cytokine mRNA Degradation in Cardiomyocytes Restrains Sterile Inflammation in Pressure-Overloaded Hearts. *Circulation*. 2020;141:667-677.
26. Kakiuchi N, Yoshida K, Uchino M, Kihara T, Akaki K, Inoue Y, Kawada K, Nagayama S, Yokoyama A, Yamamoto S, Matsuura M, Horimatsu T, Hirano T, Goto N, Takeuchi Y, Ochi Y, Shiozawa Y, Kogure Y, Watatani Y, Fujii Y, Kim SK, Kon A, Kataoka K, Yoshizato T, Nakagawa MM, Yoda A, Nanya Y, Makishima H, Shiraishi Y, Chiba K, Tanaka H, Sanada M, Sugihara E, Sato T, Maruyama T, Miyoshi H, Taketo MM, Oishi J, Inagaki R, Ueda Y, Okamoto S, Okajima H, Sakai Y, Sakurai T, Haga H, Hirota S, Ikeuchi H, Nakase H, Marusawa H, Chiba T, Takeuchi O, Miyano S, Seno H and Ogawa S. Frequent mutations that converge on the NFKBIZ pathway in ulcerative colitis. *Nature*. 2020;577:260-+.
27. Nakatsuka Y, Yaku A, Handa T, Vandenbon A, Hikichi Y, Motomura Y, Sato A, Yoshinaga M, Tanizawa K, Watanabe K, Hirai T, Chin K, Suzuki Y, Uehata T, Mino T, Tsujimura T, Moro K and Takeuchi O. Profibrotic function of pulmonary group 2

innate lymphoid cells is controlled by regnase-1. *Eur Respir J*. 2021;57.

28. Nanki K, Fujii M, Shimokawa M, Matano M, Nishikori S, Date S, Takano A, Toshimitsu K, Ohta Y, Takahashi S, Sugimoto S, Ishimaru K, Kawasaki K, Nagai Y, Ishii R, Yoshida K, Sasaki N, Hibi T, Ishihara S, Kanai T and Sato T. Somatic inflammatory gene mutations in human ulcerative colitis epithelium. *Nature*. 2020;577:254-+.
29. Nagaya N, Nishikimi T, Uematsu M, Satoh T, Kyotani S, Sakamaki F, Kakishita M, Fukushima K, Okano Y, Nakanishi N, Miyatake K and Kangawa K. Plasma brain natriuretic peptide as a prognostic indicator in patients with primary pulmonary hypertension. *Circulation*. 2000;102:865-870.
30. Nagaya N, Uematsu M, Satoh T, Kyotani S, Sakamaki F, Nakanishi N, Yamagishi M, Kunieda T and Miyatake K. Serum uric acid levels correlate with the severity and the mortality of primary pulmonary hypertension. *Am J Respir Crit Care Med*. 1999;160:487-92.
31. Dobosz E, Lorenz G, Ribeiro A, Wurf V, Wadowska M, Kotlinowski J, Schmaderer C, Potempa J, Fu M, Koziel J and Lech M. Murine myeloid cell MCPIP1 suppresses autoimmunity by regulating B-cell expansion and differentiation. *Dis Model Mech*. 2021;14.
32. Bueno-Beti C, Hadri L, Hajjar RJ and Sassi Y. The Sugen 5416/Hypoxia Mouse Model of Pulmonary Arterial Hypertension. *Methods Mol Biol*. 2018;1816:243-252.
33. Browaeys R, Saelens W and Saeys Y. NicheNet: modeling intercellular communication by linking ligands to target genes. *Nat Methods*. 2020;17:159-162.
34. Trankle CR, Canada JM, Kadariya D, Markley R, De Chazal HM, Pinson J, Fox A, Van Tassell BW, Abbate A and Grinnan D. IL-1 Blockade Reduces Inflammation in Pulmonary Arterial Hypertension and Right Ventricular Failure: A Single-Arm, Open-Label, Phase IB/II Pilot Study. *Am J Respir Crit Care Med*. 2019;199:381-384.
35. Ghofrani HA, Morrell NW, Hoeper MM, Olschewski H, Peacock AJ, Barst RJ, Shapiro S, Golpon H, Toshner M, Grimminger F and Pascoe S. Imatinib in Pulmonary Arterial Hypertension Patients with Inadequate Response to Established Therapy. *Am J Resp Crit Care*. 2010;182:1171-1177.
36. Hoeper MM, Barst RJ, Bourge RC, Feldman J, Frost AE, Galie N, Gomez-Sanchez MA, Grimminger F, Grunig E, Hassoun PM, Morrell NW, Peacock AJ, Satoh T, Simonneau G, Tapson VF, Torres F, Lawrence D, Quinn DA and Ghofrani HA. Imatinib Mesylate as Add-on Therapy for Pulmonary Arterial Hypertension

Results of the Randomized IMPRES Study. *Circulation*. 2013;127:1128-+.

37. Abe K, Toba M, Alzoubi A, Ito M, Fagan KA, Cool CD, Voelkel NF, McMurtry IF and Oka M. Formation of Plexiform Lesions in Experimental Severe Pulmonary Arterial Hypertension. *Circulation*. 2010;121:2747-2754.
38. Vitali SH, Hansmann G, Rose C, Fernandez-Gonzalez A, Scheid A, Mitsialis SA and Kourembanas S. The Sugen 5416/hypoxia mouse model of pulmonary hypertension revisited: long-term follow-up. *Pulm Circ*. 2014;4:619-629.
39. Dai Z, Li M, Wharton J, Zhu MM and Zhao YY. Prolyl-4 Hydroxylase 2 (PHD2) Deficiency in Endothelial Cells and Hematopoietic Cells Induces Obliterative Vascular Remodeling and Severe Pulmonary Arterial Hypertension in Mice and Humans Through Hypoxia-Inducible Factor-2alpha. *Circulation*. 2016;133:2447-58.
40. Kapitsinou PP, Rajendran G, Astleford L, Michael M, Schonfeld MP, Fields T, Shay S, French JL, West J and Haase VH. The Endothelial Prolyl-4-Hydroxylase Domain 2/Hypoxia-Inducible Factor 2 Axis Regulates Pulmonary Artery Pressure in Mice. *Mol Cell Biol*. 2016;36:1584-94.
41. Sibomana JP, Campeche A, Carvalho-Filho RJ, Correa RA, Duani H, Pacheco Guimaraes V, Hilton JF, Kassa B, Kumar R, Lee MH, Loureiro CMC, Mazimba S, Mickael C, Oliveira RKF, Ota-Arakaki JS, Rezende CF, Silva LCS, Sinkala E, Ahmed HY and Graham BB. Schistosomiasis Pulmonary Arterial Hypertension. *Front Immunol*. 2020;11:608883.
42. Whitsett JA and Alenghat T. Respiratory epithelial cells orchestrate pulmonary innate immunity. *Nat Immunol*. 2015;16:27-35.
43. Hameed AG, Arnold ND, Chamberlain J, Pickworth JA, Paiva C, Dawson S, Cross S, Long L, Zhao L, Morrell NW, Crossman DC, Newman CMH, Kiely DG, Francis SE and Lawrie A. Inhibition of tumor necrosis factor-related apoptosis-inducing ligand (TRAIL) reverses experimental pulmonary hypertension. *J Exp Med*. 2012;209:1919-1935.
44. Akaki K, Ogata K, Yamauchi Y, Iwai N, Tse KM, Hia F, Mochizuki A, Ishihama Y, Mino T and Takeuchi O. IRAK1-dependent Regnase-1-14-3-3 complex formation controls Regnase-1-mediated mRNA decay. *Elife*. 2021;10:e71966.
45. Iwasaki H, Takeuchi O, Teraguchi S, Matsushita K, Uehata T, Kuniyoshi K, Satoh T, Saitoh T, Matsushita M, Standley DM and Akira S. The IkappaB kinase complex regulates the stability of cytokine-encoding mRNA induced by TLR-IL-1R by controlling degradation of regnase-1. *Nat Immunol*. 2011;12:1167-75.
46. Jeltsch KM, Hu DS, Brenner S, Zoller J, Heinz GA, Nagel D, Vogel KU,

Rehage N, Warth SC, Edelmann SL, Gloury R, Martin N, Lohs C, Lech M, Stehklein JE, Geerlof A, Kremmer E, Weber A, Anders HJ, Schmitz I, Schmidt-Supprian M, Fu MG, Holtmann H, Krappmann D, Ruland J, Kallies A, Heikenwalder M and Heissmeyer V. Cleavage of roquin and regnase-1 by the paracaspase MALT1 releases their cooperatively repressed targets to promote T(H)17 differentiation. *Nat Immunol*. 2014;15:1079-1089.

47. Clausen BE, Burkhardt C, Reith W, Renkawitz R and Forster I. Conditional gene targeting in macrophages and granulocytes using LysMcre mice. *Transgenic Res*. 1999;8:265-277.
48. Schneider CA, Rasband WS and Eliceiri KW. NIH Image to ImageJ: 25 years of image analysis. *Nat Methods*. 2012;9:671-5.
49. Afgan E, Baker D, Batut B, van den Beek M, Bouvier D, Cech M, Chilton J, Clements D, Coraor N, Gruning BA, Guerler A, Hillman-Jackson J, Hiltemann S, Jalili V, Rasche H, Soranzo N, Goecks J, Taylor J, Nekrutenko A and Blankenberg D. The Galaxy platform for accessible, reproducible and collaborative biomedical analyses: 2018 update. *Nucleic Acids Res*. 2018;46:W537-W544.
50. Martin M. Cutadapt removes adapter sequences from high-throughput sequencing reads. *EMBnetjournal*. 2011;17:10.
51. Kim D, Langmead B and Salzberg SL. HISAT: a fast spliced aligner with low memory requirements. *Nat Methods*. 2015;12:357-60.
52. Liao Y, Smyth GK and Shi W. featureCounts: an efficient general purpose program for assigning sequence reads to genomic features. *Bioinformatics*. 2014;30:923-30.
53. Ritchie ME, Phipson B, Wu D, Hu Y, Law CW, Shi W and Smyth GK. limma powers differential expression analyses for RNA-sequencing and microarray studies. *Nucleic Acids Res*. 2015;43:e47.
54. Subramanian A, Tamayo P, Mootha VK, Mukherjee S, Ebert BL, Gillette MA, Paulovich A, Pomeroy SL, Golub TR, Lander ES and Mesirov JP. Gene set enrichment analysis: a knowledge-based approach for interpreting genome-wide expression profiles. *Proc Natl Acad Sci U S A*. 2005;102:15545-50.
55. Liberzon A, Subramanian A, Pinchback R, Thorvaldsdottir H, Tamayo P and Mesirov JP. Molecular signatures database (MSigDB) 3.0. *Bioinformatics*. 2011;27:1739-40.

Figure legends

Figure 1. Regnase-1 mRNA expression was decreased in PH patients

A, The expression of *ZC3H12A* mRNA in the PBMCs in PH patients (n=77) and HV (n=77). **B,** Distribution of *ZC3H12A* expression levels in PH patients classified by WHO functional class (WHO-FC) I-II (n=33), WHO-FC III-IV (n=44) and HV (n=77). **C,** Kaplan-Meier analysis of event-free survival of PH patients divided into lower or higher expression levels of *ZC3H12A* by mean value of *ZC3H12A* expression. Major clinical events were defined as death, lung transplantation, and hospitalization for right heart failure. The log-rank test was used for the analysis. **D,** Correlation between the *ZC3H12A* expression in PH patient PBMCs and mPAP. **E,** The expression of *ZC3H12A* in PH patients with higher (≥30) (n=42) and lower (<30) RVEF (n=14). **F,** Correlation between the *ZC3H12A* expression in PH patient PBMCs and plasma BNP concentrations. **G,** The expression of *ZC3H12A* in PH patient PBMCs with lower (< 100) and higher (≥ 100) BNP. **H through I**, Correlation between the *ZC3H12A* expression in PH patient PBMCs and serum uric acid concentrations (**H**) and CRP levels **(I)**. **J,** The expression of *ZC3H12A* in PH patient PBMCs with lower (<0.3) and higher (≥0.3) CRP. **K,** PH patients who underwent PAH-specific medications (n=53) were divided into low mPAP (<45mmHg) and high mPAP (≥45mmHg) groups, and compared the expression of *ZC3H12A*. **P*<0.05, ***P*<0.01, ****P*<0.001, *****P*<0.0001. Unpaired Student's t test and One-way ANOVA with Tukey's multiple comparisons test were used for analysis. Correlation analysis was performed with Pearson's linear correlation (R = Pearson's linear correlation coefficient) or Spearman's rank correlation test (ρ = Spearman's rank correlation coefficient).

Figure 2. Inverse correlation between the Regnase-1 mRNA expression in PBMCs and pathogenesis of CTD-PAH

A, The expression of *ZC3H12A* in the PBMCs in PH patients with indicated groups. PoPH,

portopulmonary hypertension. **B,** Distribution of *ZC3H12A* expression levels in CTD-PAH patients classified by WHO-FC I-II (n=9), WHO-FC III-IV (n=13) and HV (n=77). **C,** Distribution of *ZC3H12A* expression levels in I/HPAH patients classified by WHO-FC I-II (n=20), WHO-FC III-IV (n=13) and HV (n=77). **D,** Association between mPAP and the *ZC3H12A* expression in CTD-PAH and I/HPAH patient PBMCs. **E,** Association between 6MWD and the *ZC3H12A* expression in CTD-PAH and I/HPAH patient PBMCs. **F,** Association between serum uric acid concentrations and the *ZC3H12A* expression in CTD-PAH and I/HPAH patient PBMCs. **G,** The expression of *ZC3H12A* in CTD-PAH and I/HPAH patient PBMCs with lower (<0.3) and higher (≥0.3) CRP. **P*<0.01, ****P*<0.001, *****P*<0.0001. Unpaired Student's t test and One-way ANOVA with Tukey's multiple comparisons test were used for the analysis. Correlation analysis was performed with Pearson's linear correlation (R = Pearson's linear correlation coefficient).

Figure 3. Spontaneous development of severe PAH in mice lacking Regnase-1 in alveolar macrophages

A, RVSP of control (n=8: n=4 *Zc3h12a*$^{fl/+}$, n=2 *Zc3h12a*$^{fl/fl}$, n=2 CD11c-Cre^{+}*Zc3h12a*$^{fl/+}$) and CD11c-Cre^{+}*Zc3h12a*$^{fl/fl}$ (n=9) mice. **B,** RV/(LV+S) ratio of control (n=9) (n=4 *Zc3h12a*$^{fl/+}$, n=3 *Zc3h12a*$^{fl/fl}$, n=2 CD11c-Cre^{+}*Zc3h12a*$^{fl/+}$) and CD11c-Cre^{+}*Zc3h12a*$^{fl/fl}$ mice at 9 wk (n=10) and 14 wk (n=10) old. **C,** Histological images of severe stenosis due to medial and intimal thickening of CD11c-Cre^{+}*Zc3h12a*$^{fl/fl}$ and control mice (9 wk). H&E staining, EVG staining and immunohistochemistry for α-SMA and von Willebrand factor (vWF) are shown. **D,** Occlusion rates of pulmonary arteries in CD11c-Cre^{+}*Zc3h12a*$^{fl/fl}$ (n=6: n=3 *Zc3h12a*$^{fl/+}$, n=2 *Zc3h12a*$^{fl/fl}$, n=1 CD11c-Cre^{+}*Zc3h12a*$^{fl/+}$) and control (n=5) mice (9 wk). **E,** Histological scoring of pulmonary arterial remodeling in control and CD11c-Cre^{+}*Zc3h12a*$^{fl/fl}$ lungs. G0; Normal, G1; Medial hypertrophy, G2; Medial hypertrophy and intimal thickening (<75%), G3; Occlusive regions (≥75% occlusion) or intimal fibrosis. **F,** A representative low-

magnification EVG image of CD11c-Cre^{+}*Zc3h12a*$^{fl/fl}$ lung and high magnification images of pulmonary arteries. (i, plexiform-like lesion; ii, medial wall thickening (G1); iii, occlusive fibrous intimal thickening (G3); iv, complex plexiform-like lesions (plexiform and aneurysm-like lesions) and thickening of the adventitia (G4)). Br indicates bronchus. **G,** H&E and EVG images of pulmonary veins with intensive inflammation in CD11c-Cre^{+}*Zc3h12a*$^{fl/fl}$ and control mice veins. **H,** RVSP of control (n = 8: n=1 *Zc3h12a*$^{fl/+}$, n=7 *Zc3h12a*$^{fl/fl}$) and *LysM*$^{Cre/+}$*Zc3h12a*$^{fl/fl}$ (n=10) mice. **I,** RV/(LV+S) ratio of control (n=8: n=1 *Zc3h12a*$^{fl/+}$, n=7 *Zc3h12a*$^{fl/fl}$) and *LysM*$^{Cre/+}$*Zc3h12a*$^{fl/fl}$ mice at 13 wk (n=10) and 20 wk (n=7) old. **J,** Occlusion rates of pulmonary arteries in *LysM*$^{Cre/+}$*Zc3h12a*$^{fl/fl}$ (n=5) and control (n=5: *Zc3h12a*$^{fl/fl}$) mice (13 wk). **K,** Histological scoring of pulmonary arterial remodeling in control at 13 wk and *LysM*$^{Cre/+}$*Zc3h12a*$^{fl/fl}$ lungs at 13 wk (n=5) and 20 wk (n=5). G0; Normal, G1; Medial hypertrophy, G2; Medial hypertrophy and intimal thickening (<75%), G3; Occlusive regions (≥75% occlusion) or intimal fibrosis. **L,** A representative low-magnification EVG image of *LysM*$^{Cre/+}$*Zc3h12a*$^{fl/fl}$ lung and high magnification images of pulmonary arteries (20 wk). **(**i,iii, medial wall thickening (G1); ii,v; progressive fibrous vascular remodeling (G3); iv, complex plexiform-like lesions (aneurysm-like lesions) and thickening of the adventitia**) M,** H&E and EVG images of pulmonary veins with moderate inflammation in *LysM*$^{Cre/+}$*Zc3h12a*$^{fl/fl}$ and control mice (20 wk). Br indicates bronchus. Scale bar, 50 μm, otherwise indicated in the image. Data are mean ± SD. Unpaired Student's t test or One way ANOVA with Tukey's multiple comparisons test was used for the analysis. **P*<0.05, ***P*<0.01, ****P*<0.001.

Figure 4. Regnase-1-deficiency in alveolar macrophages contributes to the promotion of PAH

A and **B,** RVSP (**A**) and RV/(LV+S) ratio (**B**) control (n=7) and CD11c-Cre^{+}*Zc3h12a*$^{fl/+}$ (n=9) mice under hypoxic conditions. **C**, Occlusion rates of pulmonary arteries of

control (n=5) and CD11c-Cre^{+}*Zc3h12a*$^{fl/+}$ (n=10) mice under hypoxic conditions. Vessels were assessed for at least 30 small pulmonary arteries (<100 μm in diameter) for each mouse. **D** and **E,** RVSP (**D**) and RV/(LV+S) ratio (**E**) of control (n=4) and *LysM*$^{Cre/+}$*Zc3h12a*$^{fl/+}$ mice (n=6) housed under hypoxic conditions. **F**, Occlusion rates of pulmonary arteries of control (n=4) and *LysM*$^{Cre/+}$*Zc3h12a*$^{fl/+}$ mice (n=5) housed under hypoxic conditions. **G** through **I,** RVSP (**G**), RV/(LV+S) (**H**) and occlusion rates of pulmonary arteries (**I**) of control (n=5) and CD11c-Cre^{+}*Zc3h12a*$^{fl/fl}$*Rag2*$^{-/-}$ mice (n=6) (16 wk). **J,** Histological scoring of pulmonary arterial remodeling in CD11c-Cre^{+}*Zc3h12a*$^{fl/fl}$ (n=4) and CD11c-Cre^{+}*Zc3h12a*$^{fl/fl}$*Rag2*$^{-/-}$ (n= 5) lungs (16 wk). **K,** A representative EVG image of CD11c-Cre^{+}*Zc3h12a*$^{fl/fl}$*Rag2*$^{-/-}$ lung (8 months) and pulmonary arteries with higher magnification. (i,iv,v,vi occlusive intimal thickening (G3); ii, intimal thickening (partial occlusion) (G2); iii: complex plexiform-like lesions (aneurysm-like lesions) and thickening of the adventitia) Br indicates bronchus. Scale bar, 50 μm otherwise indicated in the image. **L,** A scheme for the treatment of CD11c-Cre^{+}*Zc3h12a*$^{fl/fl}$*Rag2*$^{-/-}$ mice with clodronate liposome (CL). **M,** Numbers of alveolar and interstitial macrophages in the right lung with or without the CL treatment. Mean + SD. is shown. **N** and **O**, Representative EVG images **(N)** and occlusion rates **(O)** of pulmonary arteries from clodronate-treated CD11c-Cre^{+}*Zc3h12a*$^{fl/fl}$*Rag2*$^{-/-}$ mice are shown. Scale bar, 50 μm. Data are mean ± SD. Unpaired Student's t test was used for the analysis. **P*<0.05, ***P*<0.01, ****P*<0.001.

Figure 5. Analysis of ligand-target linkage between Regnase-1-deficient alveolar macrophages and pulmonary arteries

A, Experimental schemes for the transcriptome analysis of pulmonary arteries and alveolar macrophages from CD11c-Cre^{+}*Zc3h12a*$^{fl/fl}$ and control mice. **B,** GSEA analysis for the gene sets involved in cell cycling ("Cell Cycle" and "E2F target") on the transcriptome data from pulmonary arteries. **C,** GO processes highly enriched in genes

increased in CD11c-Cre^{+}*Zc3h12a*$^{fl/fl}$ pulmonary arteries. **D,** KEGG pathway analysis for genes increased in CD11c-Cre^{+}*Zc3h12a*$^{fl/fl}$ pulmonary arteries. **E** and **F,** Heatmaps of the expression of cytokines **(E)** and M1 and M2 macrophage signature genes **(F)** in alveolar macrophages from CD11c-Cre^{+}*Zc3h12a*$^{fl/fl}$ alveolar macrophages. **G,** Ligand-target linkage analysis between alveolar macrophages and pulmonary arteries by using the NicheNet method. Ligand activity prediction on the gene sets upregulated in CD11c-Cre^{+}*Zc3h12a*$^{fl/fl}$ pulmonary arteries by using the NicheNet, and Ligand–target matrix denoting the regulatory potential between Regnase-1-deficient alveolar macrophage-ligands and target genes in pulmonary arteries.

Figure 6. Regnase-1 protects against the progression of PAH by degrading *Il6* and *Pdgf* mRNAs.

A, Luciferase reporter analysis for Regnase-1-mediated suppression of gene expression through the 3′UTR sequence of the indicated genes. Either an empty plasmid, murine Regnase-1, or a nuclease-dead mutant (D141N) were transfected into HEK293T cells together with reporter plasmids, and luciferase activity was measured on day 2 (n=3). Data representative of two independent studies is shown. Mean + SD. is shown. **B** through **G**, Amelioration of PAH in CD11c-Cre^{+}*Zc3h12a*$^{fl/fl}$ mice by suppressing the IL-6 signaling. Schematic presentation of experimental protocol for the treatment of CD11c-Cre^{+}*Zc3h12a*$^{fl/fl}$ mice with MR16-1 (anti-IL-6 receptor antibody) or control IgG **(B)**. Assessment of RVSP **(C)**, RV/(LV+S) ratio **(D)**, EVG images **(E)**, pulmonary arterial occlusion rates **(F)** and histological scoring of pulmonary arterial remodeling **(G)** of CD11c-Cre^{+}*Zc3h12a*$^{fl/fl}$ mice treated with MR16-1 (n=6) or control IgG (n=8). Scale bar, 50 μm. **H** through **M,** Alleviation of PAH in CD11c-Cre^{+}*Zc3h12a*$^{fl/fl}$ mice by inhibiting PDGF, but not IL-1, signaling. Schematic presentation of experimental protocol for the treatment of CD11c-Cre^{+}*Zc3h12a*$^{fl/fl}$ mice with anakinra (IL-1 receptor inhibitor) or imatinib (PDGF receptor inhibitor) **(H)**. Assessment of RVSP **(I)**,

RV/(LV+S) ratio **(J)**, EVG images **(K)**, pulmonary arterial occlusion rates **(L)** and histological scoring of pulmonary arterial remodeling **(M)** of CD11c-Cre^{+}*Zc3h12a*$^{fl/fl}$ mice treated with anakinra (n=7), imatinib (n=10) or control vehicle (n=8). Scale bar, 50 μm. Data are mean ± SD. Unpaired Student's t test and One way ANOVA with Dunnett's multiple comparisons test were used for the analysis **P*<0.05, ***P*<0.01, ****P*<0.001

Table 1. Characteristics of the study population

			ZC3H12A mRNA expression			
	HV (n = 77)	**PH** (n = 77)	**Quartile 1** (n = 19)	**Quartile 2** (n = 20)	**Quartile 3** (n = 19)	**Quartile 4** (n = 19)
ZC3H12A mRNA expression	0.01003 (0.01222-0.00855)	0.00680 (0.00493-0.00907)	0.00385 (0.00319-0.00410)	0.00615 (0.00532-0.00648)	0.00776 (0.00744-0.00809)	0.01060 (0.00969-0.01184)
Age, years (IQR)	44 (32-52)	48 (36-59)	54 (28-63)	42 (34-54)	49 (40-63)	48 (37-58)
Female, n (%)	52 (68)	58 (75)	11 (58)	16 (80)	16 (84)	15 (79)
PH subgroups						
Idiopathic or heritable PAH (I/HPAH), n	—	33	8	12	4	9
Connective tissue disease associated PAH (CTD-PAH), n	—	22	4	4	7	7
Congenital heart disease associated PAH (CHD-PAH), n	—	6	0	2	4	0
Portopulmonary hypertension (PoPH), n	—	5	0	1	2	2
Chronic thromboembolic PH (CTEPH), n	—	4	3	1	0	0
Drug-induced PAH, n	—	2	0	0	1	1
Groups 3&5, n	—	5	4	0	1	0
-Group 3 PH, n		3	2	0	1	0
-Castleman's disease, n		1	1	0	0	0
-Down's syndrome, n		1	1	0	0	0
WHO-FC, n (%)	—					
I		2 (2.5)	1 (5)	0 (0)	0 (0)	1 (5)
II		30 (39)	3 (16)	11 (55)	6 (32)	10 (53)
III		43 (56)	13 (68)	9 (45)	13 (68)	8 (42)
IV		2 (2.5)	2 (11)	0 (0)	0 (0)	0 (0)
Uric acid, mg/dl	—	5.8 ± 1.5	6.9 ± 1.8	5.6 ± 1.8	5.6 ± 0.7	5.0 ± 1.0
CRP, mg/dl	—	0.09 (0.03-0.35)	0.15 (0.02-0.69)	0.10 (0.02-0.35)	0.12 (0.04-0.45)	0.05 (0.02-0.14)
BNP, pg/ml	—	43.2 (16.9-124.6)	103.8 (13.0-227.1)	47.9 (19.6-118.1)	73.7 (14.0-167.0)	34.6 (18.0-54.1)
6MWD*, m	—	471± 116	467± 147	469± 103	447± 112	498± 119
RAP, mmHg	—	4.0 (2.0-5.0)	4.0 (3.0-5.0)	3.5 (2.0-6.0)	3.0 (0.0-6.0)	3.0 (2.0-5.0)
mean PAP, mmHg	—	39 ± 14	44 ± 14	37 ± 11	41 ± 14	35 ± 14
PVR, Wood Units	—	7.0 (5.3-10.7)	7.0 (5.5-12.1)	6.7 (4.4-10.2)	8.6 (5.7-14.5)	5.9 (3.9-9.0)
Cardiac index, L/min/m^2	—	2.6 ± 0.8	2.6 ± 0.9	2.7 ± 0.9	2.3 ± 0.4	2.7 ± 0.6
RVEF**, %	—	38.9 ± 10.8	33.1 ± 11.6	38.8 ± 10.9	40.5 ± 10.3	43.3 ± 8.8
No, of patients receiving PAH-specific medications	—	53 (68)	11 (58)	14 (70)	12 (63)	16 (84)
No, of Composite event, n (%)	—	12 (16)	8 (42)	1 (5)	2 (11)	1 (5)

Continuous values are expressed as mean ± SD or median (IQR). Categorical values are expressed as number and percentage; n indicates the number of patients.

P values were calculated using the chi square test for categorical variables, and the Student's t test or Welch test for continuous variables. P-value of *ZC3H12A* mRNA expression, Age, and Female between HV and

PH were p<0.0001 (unpaired Student's t-test), p=0.10 (Welch test), and p=0.28 (the chi square test), respectively.
* n= 61 (11 in Quartile 1, 19 in Quartile 2, 15 in Quartile 3, and 16 in Quartile 4.) and ** n= 56 (15 in Quartile 1, 12 in Quartile 2, 13 in Quartile 3, and 16 in Quartile 4.) because of missing data. PH patients were stratified by quartiles according to the *ZC3H12A* expression.
Abbreviations: IQR, interquartile range; HV, healthy volunteers; PH, pulmonary hypertension; PAH, pulmonary arterial hypertension; WHO-FC, World Health Organization functional class; CRP, C-reactive protein; BNP, brain natriuretic peptide; 6MWD, 6-minute walk distance; RAP, right arterial pressure; PAP, pulmonary arterial pressure; PVR, pulmonary vascular resistance; RVEF, right ventricular ejection fraction.

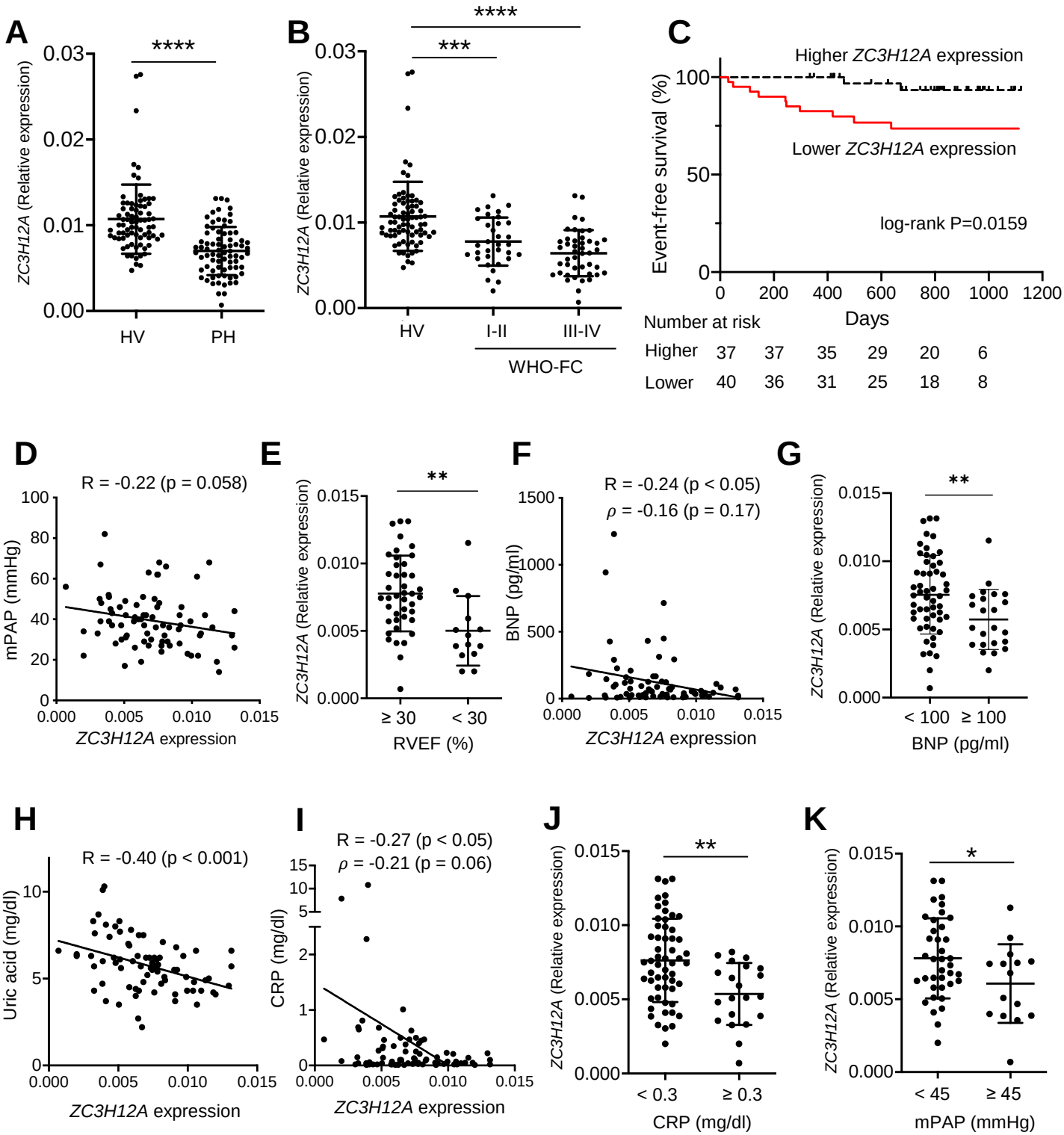
A
****
ZC3H12A (Relative expression)
0.03
0.02
0.01
0.00
HV
PH
B
****
***
ZC3H12A (Relative expression)
HV
I-II
III-IV
WHO-FC
C
Higher ZC3H12A expression
Lower ZC3H12A expression
log-rank P=0.0159
Event-free survival (%)
100
50
0
0
200
400
600
800
1000
1200
Days
Number at risk
Higher 37 37 35 29 20 6
Lower 40 36 31 25 18 8
D
R = -0.22 (p = 0.058)
mPAP (mmHg)
ZC3H12A expression
E
**
ZC3H12A (Relative expression)
≥ 30
< 30
RVEF (%)
F
R = -0.24 (p < 0.05)
ρ = -0.16 (p = 0.17)
BNP (pg/ml)
ZC3H12A expression
G
**
ZC3H12A (Relative expression)
< 100
≥ 100
BNP (pg/ml)
H
R = -0.40 (p < 0.001)
Uric acid (mg/dl)
ZC3H12A expression
I
R = -0.27 (p < 0.05)
ρ = -0.21 (p = 0.06)
CRP (mg/dl)
ZC3H12A expression
J
**
ZC3H12A (Relative expression)
< 0.3
≥ 0.3
CRP (mg/dl)
K
*
ZC3H12A (Relative expression)
< 45
≥ 45
mPAP (mmHg)

Figure 1

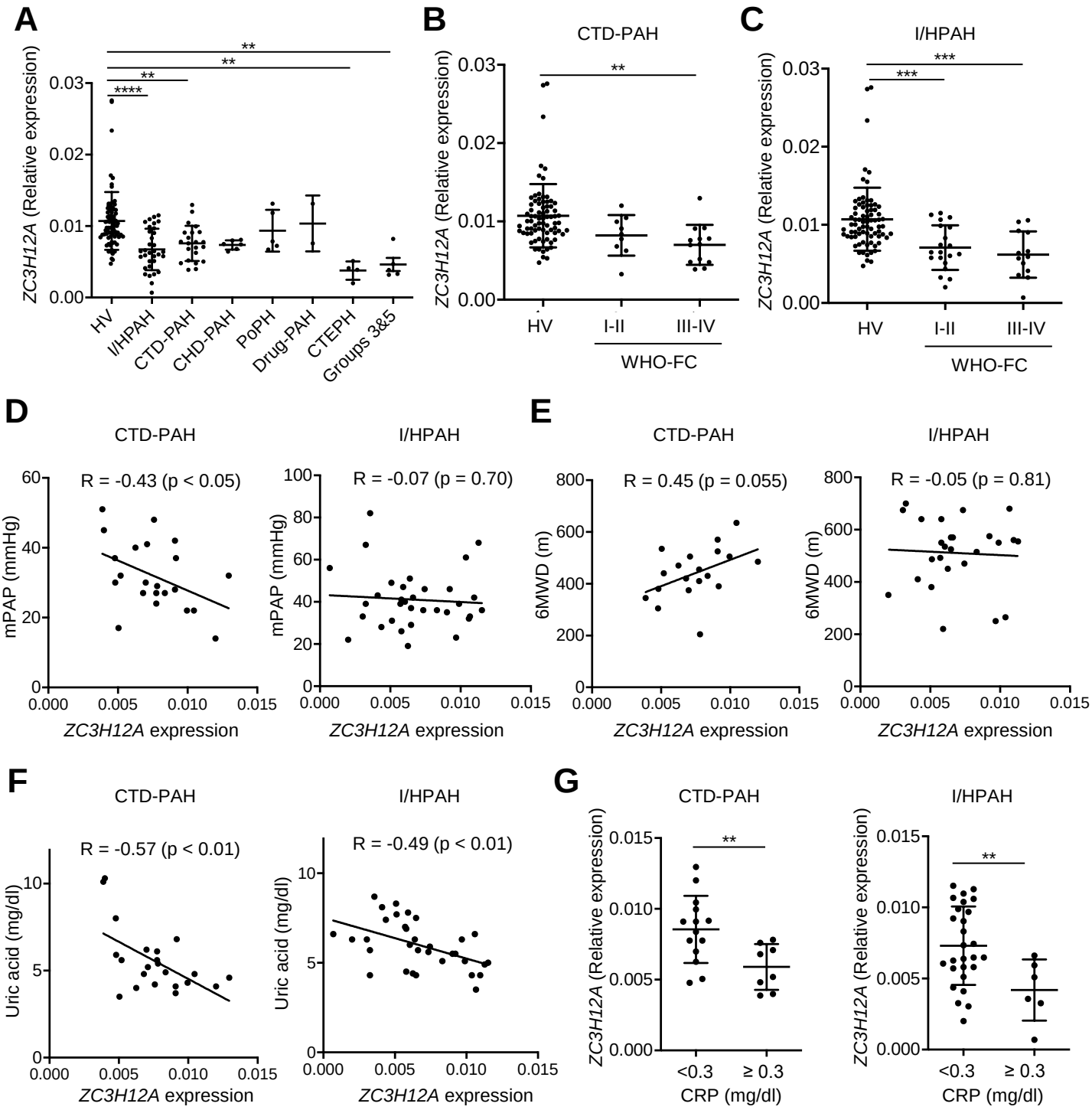
A
ZC3H12A (Relative expression)
0.03
0.02
0.01
0.00
****
**
**
**
HV
I/HPAH
CTD-PAH
CHD-PAH
PoPH
Drug-PAH
CTEPH
Groups 3&5
B
CTD-PAH
ZC3H12A (Relative expression)
**
HV
I-II
III-IV
WHO-FC
C
I/HPAH
ZC3H12A (Relative expression)
***
***
HV
I-II
III-IV
WHO-FC
D
CTD-PAH
R = -0.43 (p < 0.05)
mPAP (mmHg)
ZC3H12A expression
I/HPAH
R = -0.07 (p = 0.70)
mPAP (mmHg)
ZC3H12A expression
E
CTD-PAH
R = 0.45 (p = 0.055)
6MWD (m)
ZC3H12A expression
I/HPAH
R = -0.05 (p = 0.81)
6MWD (m)
ZC3H12A expression
F
CTD-PAH
R = -0.57 (p < 0.01)
Uric acid (mg/dl)
ZC3H12A expression
I/HPAH
R = -0.49 (p < 0.01)
Uric acid (mg/dl)
ZC3H12A expression
G
CTD-PAH
ZC3H12A (Relative expression)
**
<0.3
≥ 0.3
CRP (mg/dl)
I/HPAH
ZC3H12A (Relative expression)
**
<0.3
≥ 0.3
CRP (mg/dl)

Figure 2

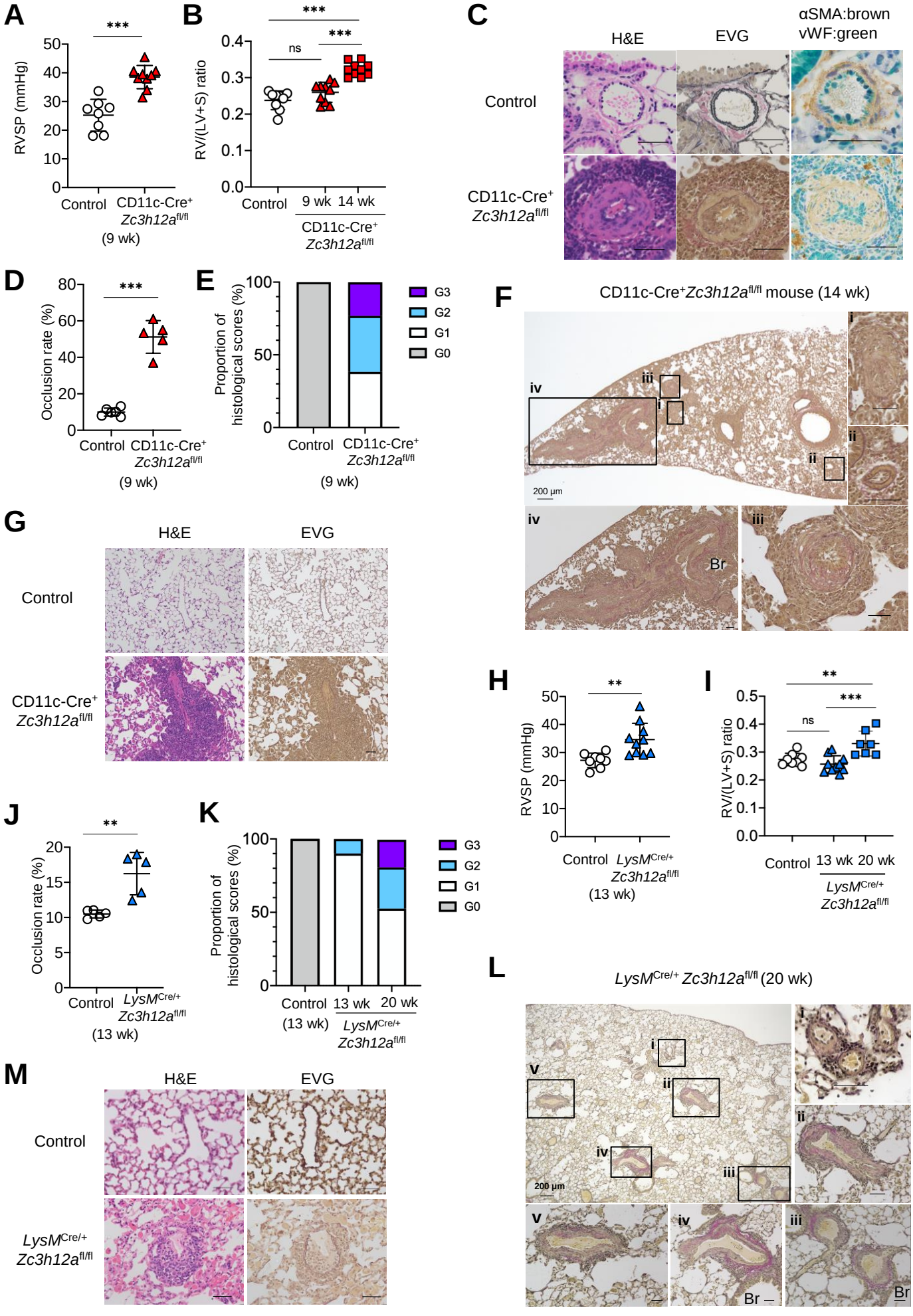
A
***
RVSP (mmHg)
50
40
30
20
10
0
Control
CD11c-Cre+ Zc3h12afl/fl
(9 wk)
B
***
ns
***
RV/(LV+S) ratio
0.4
0.3
0.2
0.1
0.0
Control
9 wk
14 wk
CD11c-Cre+ Zc3h12afl/fl
C
αSMA:brown
vWF:green
H&E
EVG
Control
CD11c-Cre+ Zc3h12afl/fl
D
***
Occlusion rate (%)
80
60
40
20
0
Control
CD11c-Cre+ Zc3h12afl/fl
(9 wk)
E
Proportion of histological scores (%)
100
50
0
G3
G2
G1
G0
Control
CD11c-Cre+ Zc3h12afl/fl
(9 wk)
F
CD11c-Cre+Zc3h12afl/fl mouse (14 wk)
i
ii
iii
iv
200 μm
Br
G
H&E
EVG
Control
CD11c-Cre+ Zc3h12afl/fl
H
**
RVSP (mmHg)
50
40
30
20
10
0
Control
LysMCre/+ Zc3h12afl/fl
(13 wk)
I
**
***
ns
RV/(LV+S) ratio
0.5
0.4
0.3
0.2
0.1
0.0
Control
13 wk
20 wk
LysMCre/+ Zc3h12afl/fl
J
**
Occlusion rate (%)
20
15
10
5
0
Control
LysMCre/+ Zc3h12afl/fl
(13 wk)
K
Proportion of histological scores (%)
100
50
0
G3
G2
G1
G0
Control
(13 wk)
13 wk
20 wk
LysMCre/+ Zc3h12afl/fl
L
LysMCre/+ Zc3h12afl/fl (20 wk)
i
ii
iii
iv
v
200 μm
Br
M
H&E
EVG
Control
LysMCre/+ Zc3h12afl/fl

Figure 3

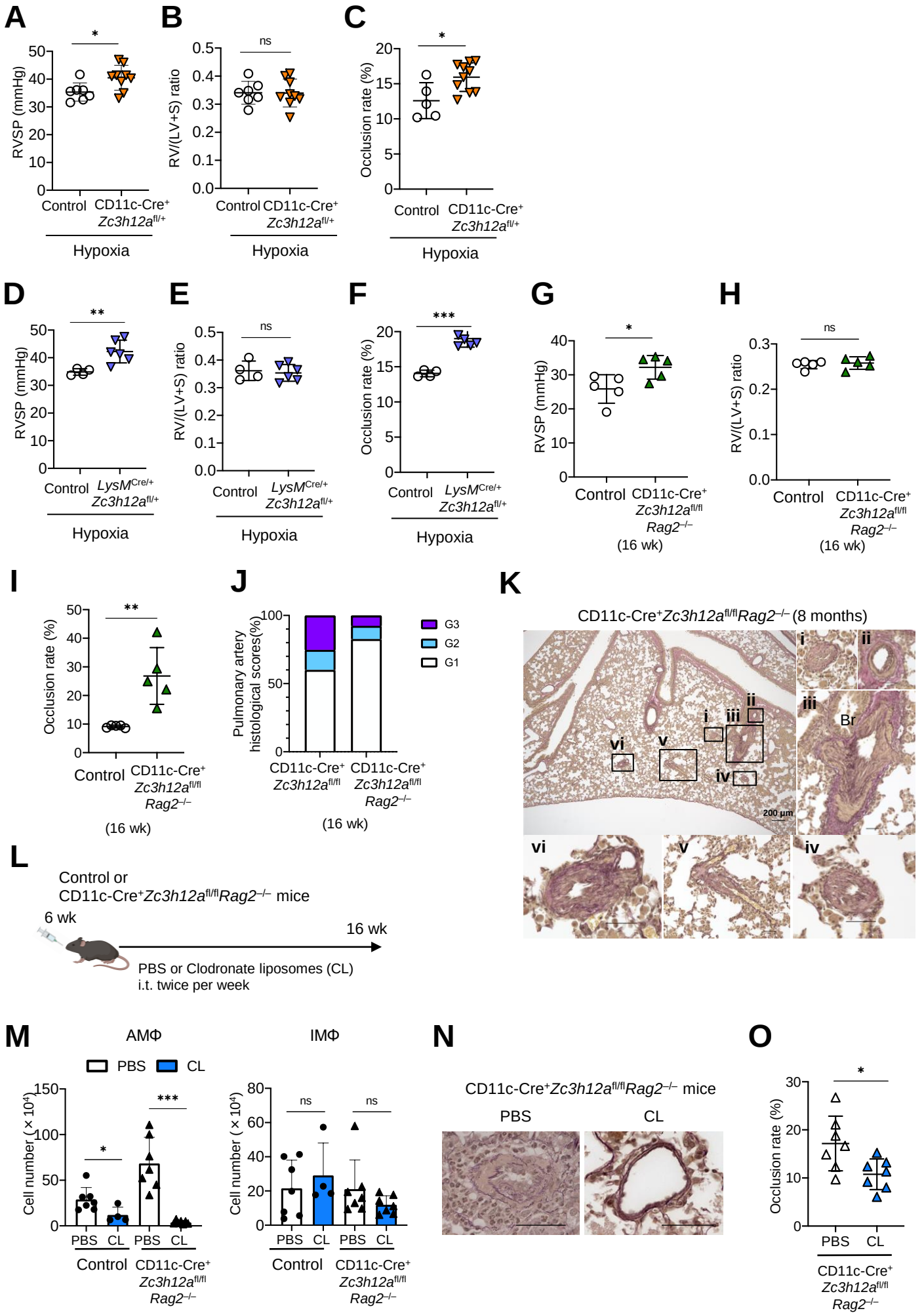
A
B
C
RVSP (mmHg)
RV/(LV+S) ratio
Occlusion rate (%)
*
ns
Control
CD11c-Cre+ Zc3h12afl/+
Hypoxia
D
E
F
G
H
**
***
LysMCre/+ Zc3h12afl/+
CD11c-Cre+ Zc3h12afl/fl Rag2−/−
(16 wk)
I
J
K
Occlusion rate (%)
Pulmonary artery histological scores(%)
G3
G2
G1
CD11c-Cre+Zc3h12afl/flRag2−/− (8 months)
i
ii
iii
iv
v
vi
Br
200 μm
L
Control or
CD11c-Cre+Zc3h12afl/flRag2−/− mice
6 wk
16 wk
PBS or Clodronate liposomes (CL)
i.t. twice per week
M
AMΦ
IMΦ
PBS
CL
Cell number (×10⁴)
N
CD11c-Cre+Zc3h12afl/flRag2−/− mice
PBS
CL
O
Occlusion rate (%)

Figure 4

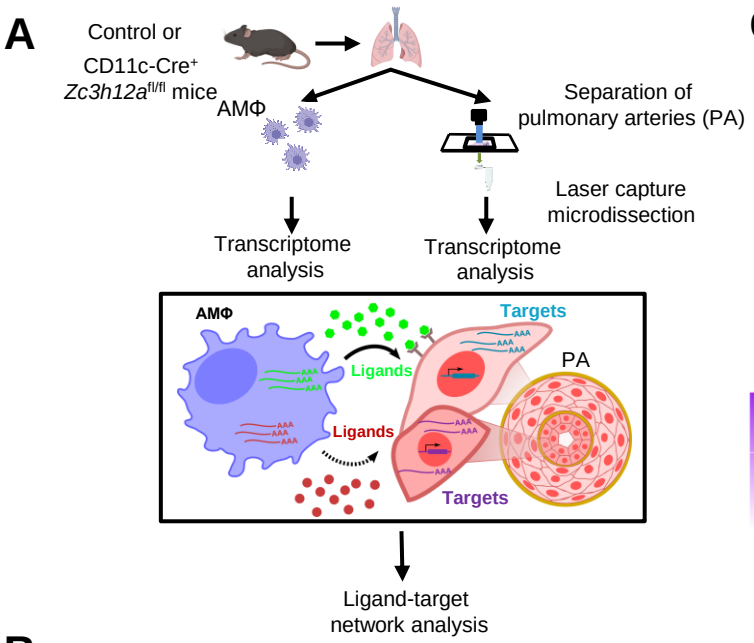

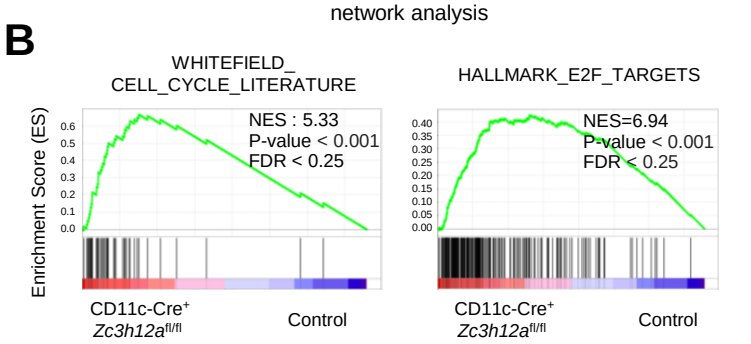

C

GO processes	P value
immune response	9.06×10^{-156}
immune system process	1.14×10^{-151}
defense response	1.51×10^{-105}
regulation of immune system process	1.17×10^{-100}
response to other organism	7.08×10^{-93}

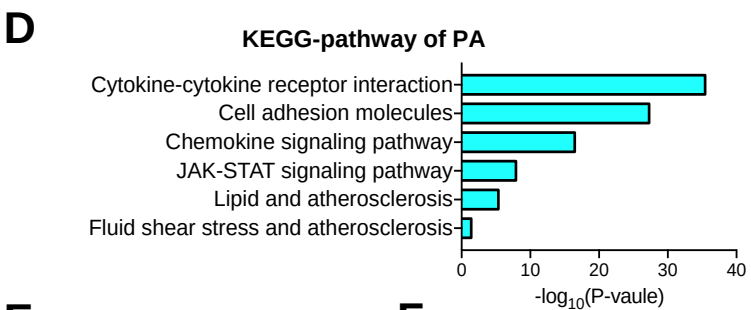

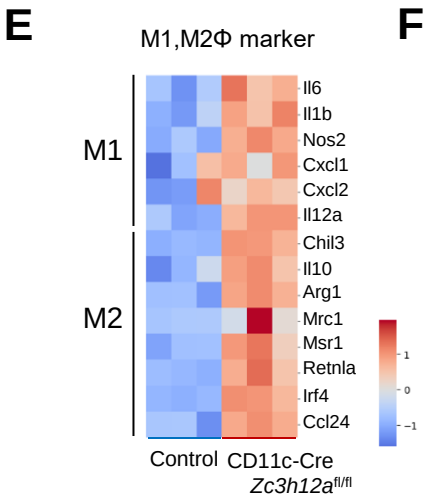

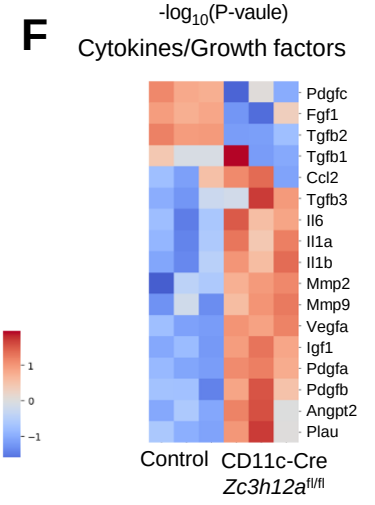

Figure 5

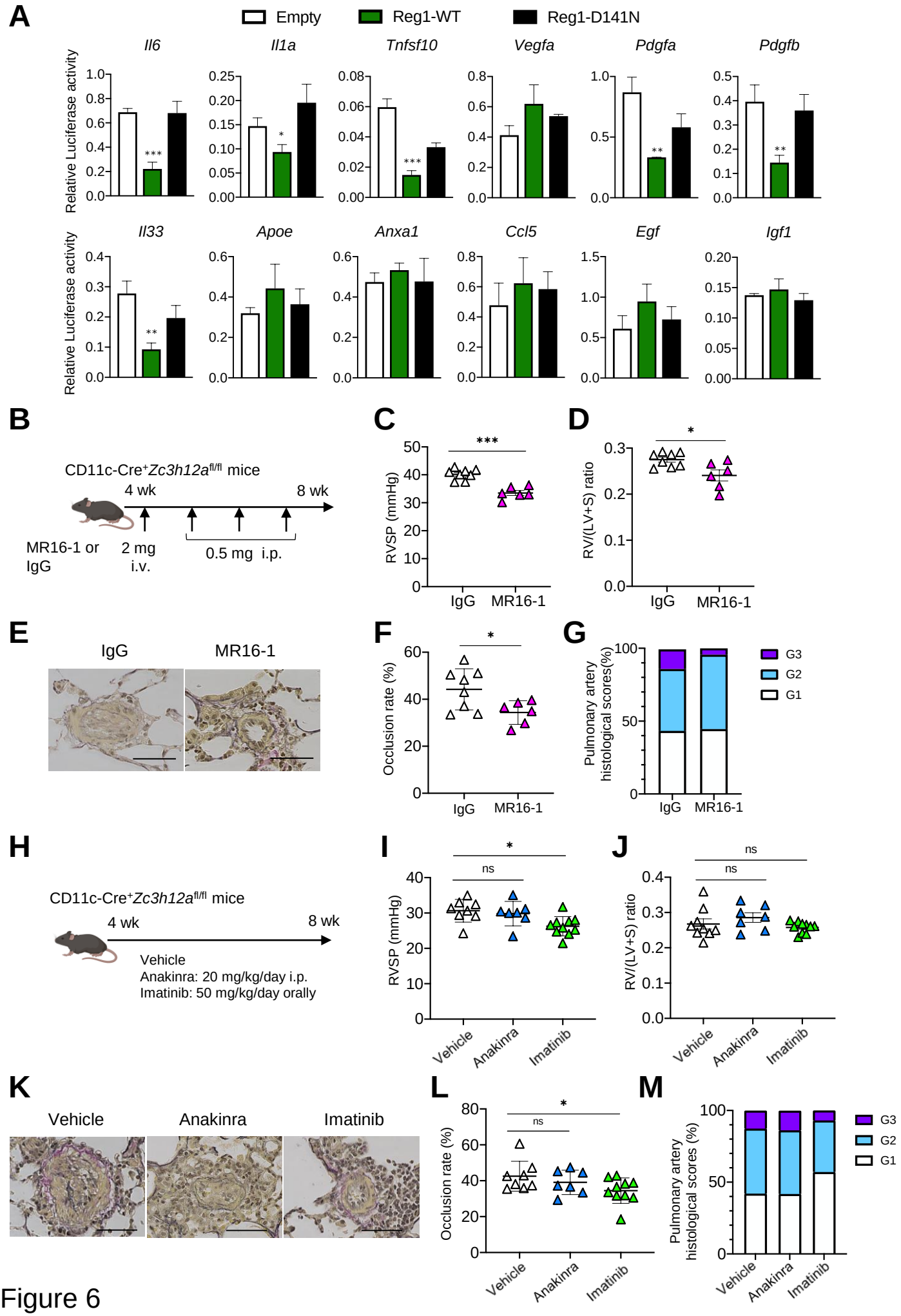
A
Empty
Reg1-WT
Reg1-D141N
Il6
Il1a
Tnfsf10
Vegfa
Pdgfa
Pdgfb
Il33
Apoe
Anxa1
Ccl5
Egf
Igf1
Relative Luciferase activity
B
CD11c-Cre+Zc3h12afl/fl mice
4 wk
8 wk
MR16-1 or IgG
2 mg i.v.
0.5 mg i.p.
C
RVSP (mmHg)
IgG
MR16-1
D
RV/(LV+S) ratio
E
IgG
MR16-1
F
Occlusion rate (%)
G
Pulmonary artery histological scores(%)
G3
G2
G1
H
CD11c-Cre+Zc3h12afl/fl mice
4 wk
8 wk
Vehicle
Anakinra: 20 mg/kg/day i.p.
Imatinib: 50 mg/kg/day orally
I
RVSP (mmHg)
ns
Vehicle
Anakinra
Imatinib
J
RV/(LV+S) ratio
K
Vehicle
Anakinra
Imatinib
L
Occlusion rate (%)
M
Pulmonary artery histological scores (%)
G3
G2
G1

Figure 6